Precision Timing with the PICOSEC-MicroMegas Detector: Physics and Instrumentation

Ioannis Manthos

Laboratory of Nuclear & Particle Physics
Physics Department
Aristotle University of Thessaloniki

on behalf of the RD51 - PICOSEC Collaboration

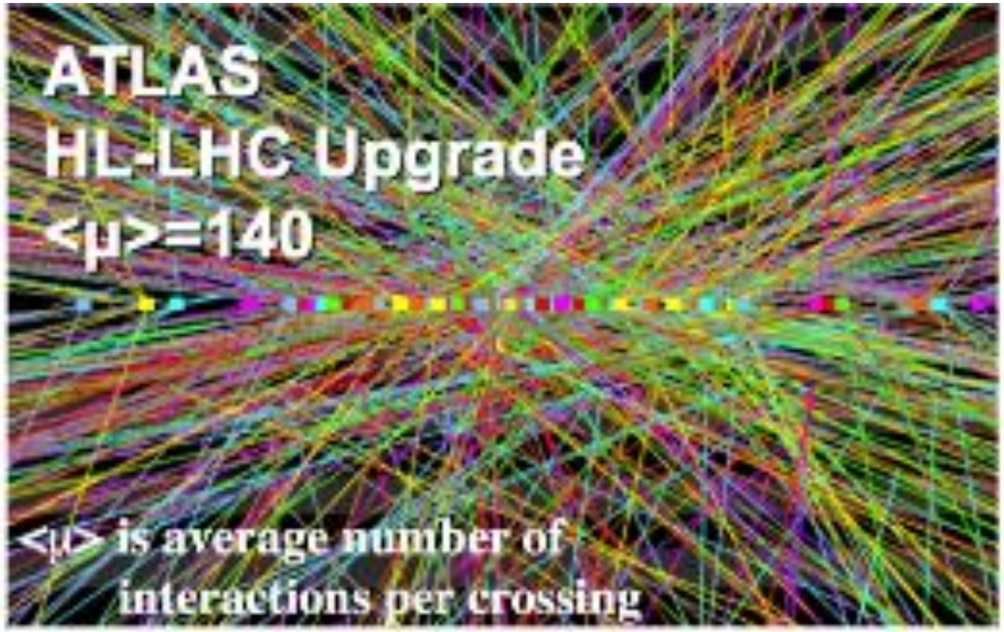

This illustrates the large number of interactions per crossing after an LHC upgrade to a luminosity of $\sim 10^{35} cm^{-2} sec^{-1}$ (ATLAS collaboration).

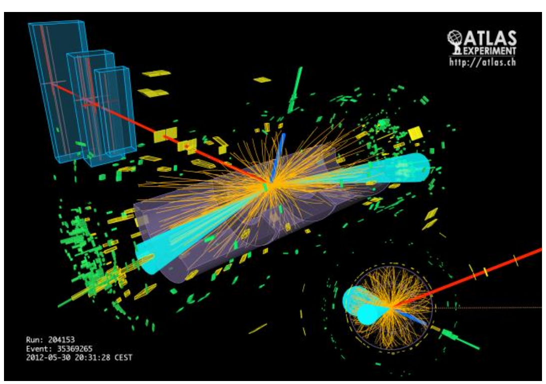

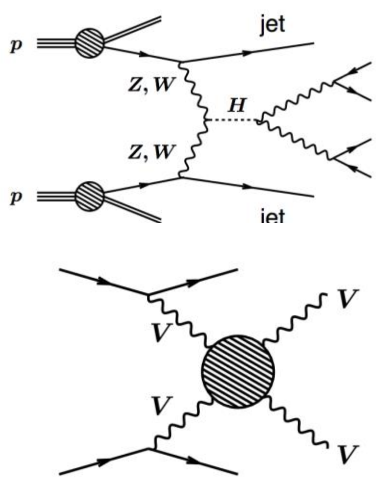

The association of the time measurement to the energy measurement is crucial for physics analysis, and requires time resolution of 20-30ps.

Existing Instrumentation:

e.g. Multi-Channel Plate (MCP) with σ_t~ 4ps but very expensive for large area coverage

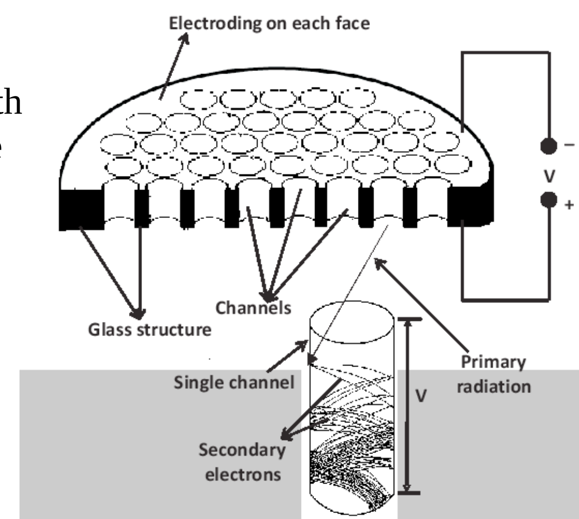

PhotoMultiplier: σ_t >800ps

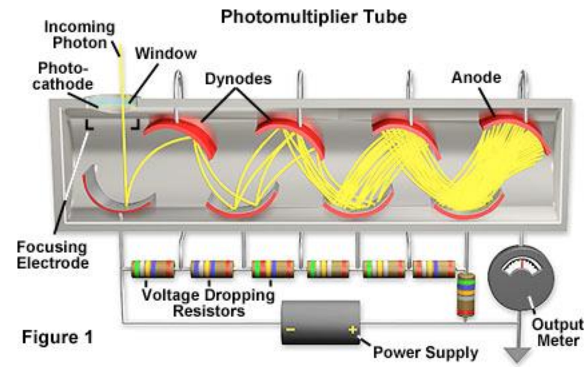

Since the hermetic approach at the LHC experiments requires large area coverage, it is natural to investigate both MicroPattern Gas and Silicon structures as candidate detector technologies. However, since the necessary time resolution for pileup mitigation is of the order of 20-30ps, both technologies require significant modification to reach the desired performance.

Large area detectors, resistant to radiation damage, with ~10ps timing capabilities will find applications in many other domains, e.g.

- particle identification in Nuclear and Particle Physics experiments
- photon's energy/speed measurements and correlations for Cosmology
- optical tracking for charge particles
- 4D tracking in the future accelerators (e.g. FCC with a center energy of ~100TeV)

MicroMegas: Micro Pattern Gaseous Chambers

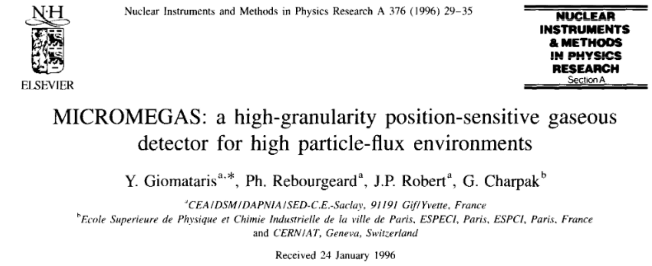

N·H
ELSEVIER
Nuclear Instruments and Methods in Physics Research A 376 (1996) 29–35
NUCLEAR INSTRUMENTS & METHODS IN PHYSICS RESEARCH Section A

MICROMEGAS: a high-granularity position-sensitive gaseous detector for high particle-flux environments

Y. Giomataris[a,*], Ph. Rebourgeard[a], J.P. Robert[a], G. Charpak[b]

[a] CEA/DSM/DAPNIA/SED-C.E.-Saclay, 91191 Gif/Yvette, France
[b] Ecole Superieure de Physique et Chimie Industrielle de la ville de Paris, ESPECI, Paris, ESPCI, Paris, France and CERN/AT, Geneva, Switzerland

Received 24 January 1996

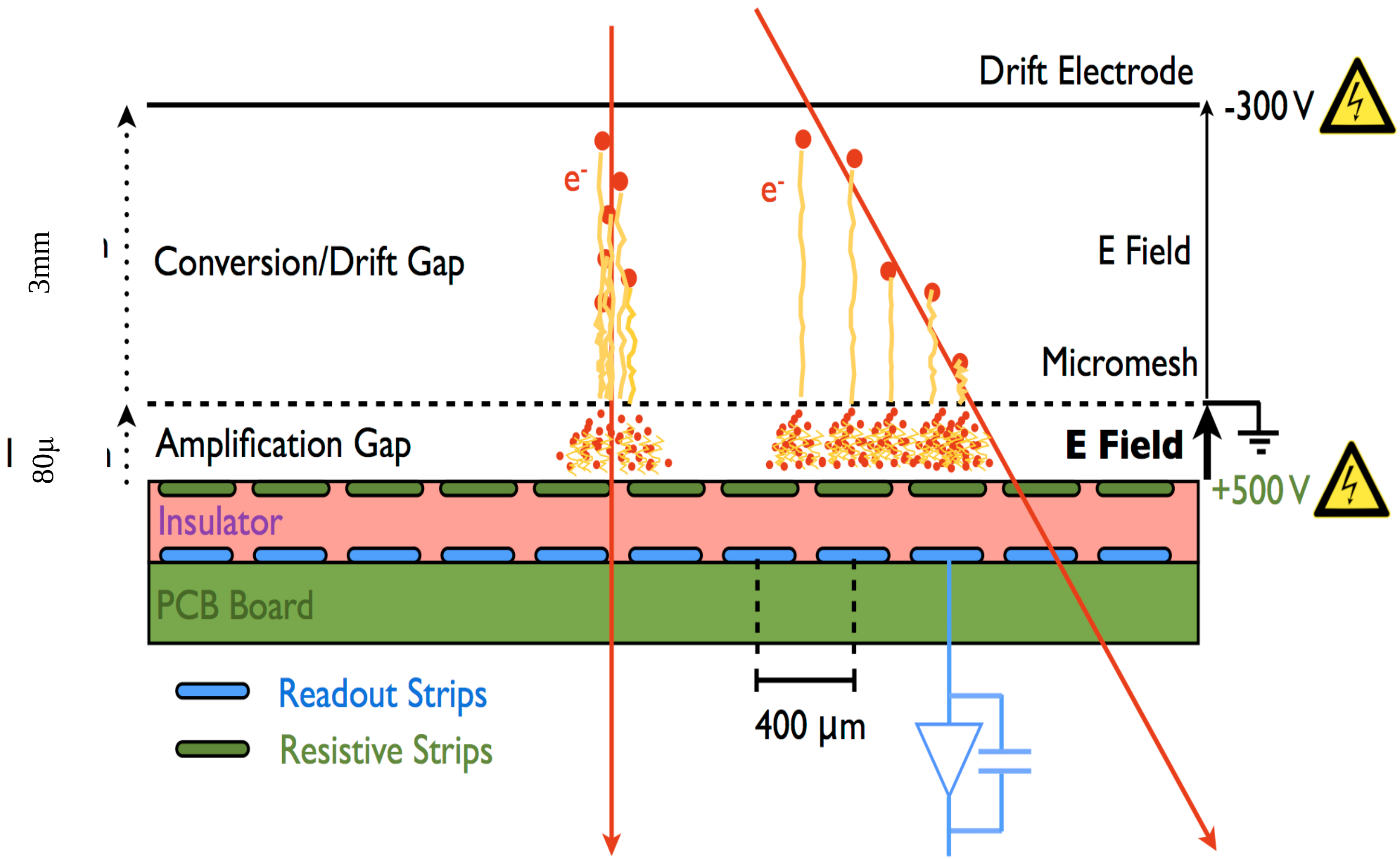

The Physics of Ionization offers the means for precise spatial measurements (high spatial resolution) but inhibits precise timing measurements

ORGANISATION EUROPÉENNE POUR LA RECHERCHE NUCLÉAIRE
CERN EUROPEAN ORGANIZATION FOR NUCLEAR RESEARCH

PRINCIPLES OF OPERATION OF MULTIWIRE
PROPORTIONAL AND DRIFT CHAMBERS

F. Sauli

Lectures given in the
Academic Training Programme of CERN
1975-1976

G E N E V A

1977

which is represented in Fig. 8, for n = 34, as a function of the coordinate across a 10 mm thick detector. If the time of detection is the time of arrival of the closest electron at one end of the gap, as is often the case, the statistics of ion-pair production set an obvious limit to the time resolution of the detector. A scale of time is also given in the figure, for a collection velocity of 5 cm/μsec typical of many gases; the FWHM of the distribution is about 5 nsec. There is no hope of improving this time resolution in a gas counter, unless some averaging over the time of arrival of all electrons is realized.

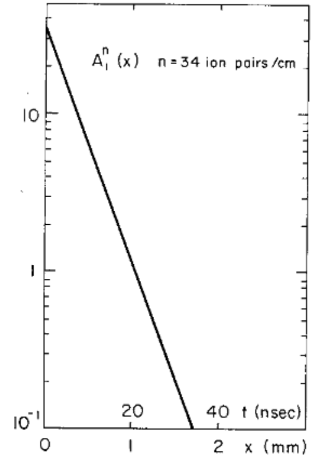

Fig. 8

Statistics of primary ion pair production: probability of finding the closest pair at a distance x from one electrode in a counter, in argon-isobutane 70-30. The corresponding electron minimum collection time is shown, for a typical drift velocity of electrons of 5 cm/μsec.

However…

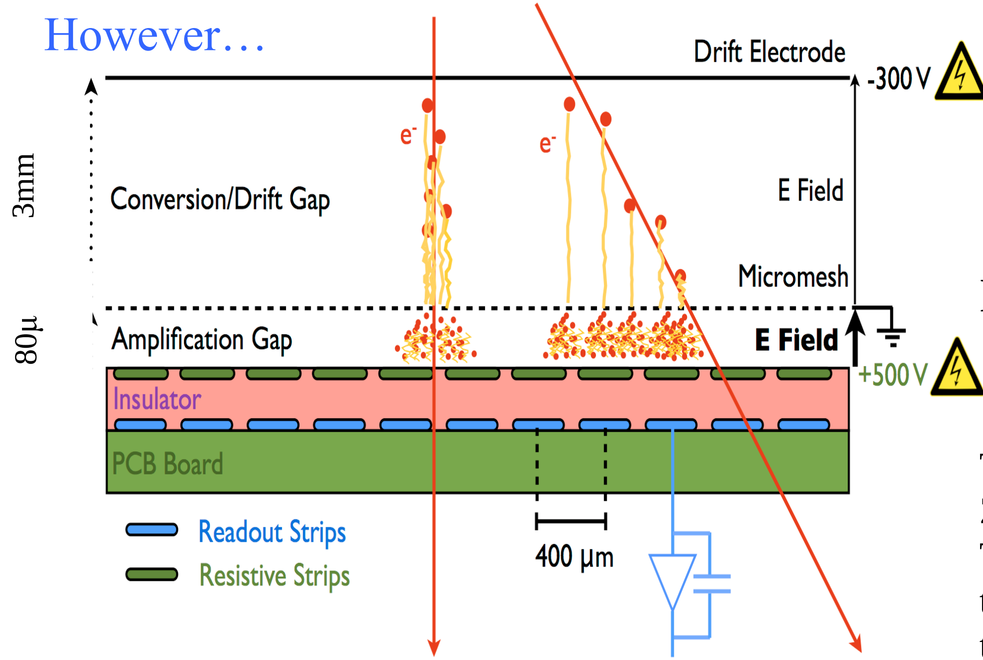

Let n be the mean number of the e-ion pairs produced by the charged particle along its track. Then the probability that k-pairs are produced by a single track is given by the Poisonian

$$P_k^n = \frac{n^k}{k!} e^{-n}$$

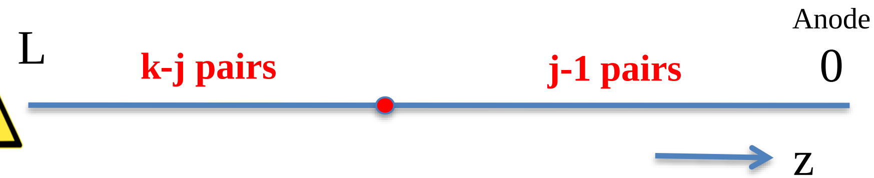

The probability that an e-ion pair has been produced at Z=z is the same for any value of Z; **p=1/L**

Then, in case that k pairs are produced, the probability that the jth pair has been produced at Z= z is given by the binomial distribution

$$D_j^k(x) = \frac{k!}{(k-j)!(j-1)!} (1-x)^{k-j} x^{j-1}$$

where **x=z/L describes the probability that a pair is produced in the region 0-z**

The probability that the jth pair has been produced at Z= z for any total number of e-ion pairs is given by

$$A_j^n(x) = \sum_{k=j}^{\infty} P_k^n D_j^k(x) = \frac{x^{j-1}}{(j-1)!} n^j e^{-nx}$$

The probability that the last pair (i.e. the closest to the edge 0) has been produced at Z= z is given by (j-1=0):

$$A_{last}^n(x) = n e^{-nx}$$

$$A_{last}^n(z) = n e^{-nz/L}$$

Using the drift velocity (V), we express the probability that the first electrons will reach the anode at time t as:

$$A_{first}^n(t) = n(V/L) e^{-nVt/L}$$

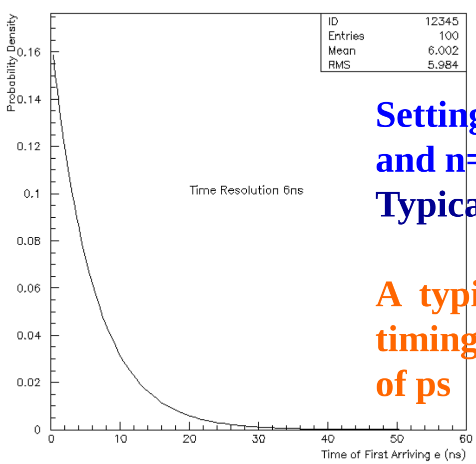

Setting typical values, i.e. V=50µm/ns and n=10 we conclude that:
Typical Time Resolution ~6ns

A typical MicroMegas cannot reach timing resolution at the level of tenths of ps

PICOSEC: Charged particle timing to 24 picosecond precision with a Micromegas based detector

J. Bortfeldt[b], F. Brunbauer[b], C. David[b], D. Desforge[a], G. Fanourakis[c], J. Franchi[b], M. Gallinaro[g], I. Giomataris[a], T. Gustavsson[a], C. Guyot[a], F.J. Iguaz[a,*], M. Kebbiri[a], P. Legou[a], J. Liu[d], M. Lupberger[b], O. Maillard[a], I. Manthos[e], H. Müller[b], V. Niaouris[e], E. Oliveri[b], T. Papaevangelou[a], K. Paraschou[e], M. Pomorski[a], B. Qi[d], F. Resnati[b], L. Ropelewski[b], D. Sampsonidis[e], T. Schneider[b], P. Schwemling[a], L. Sohl[b], M. van Stenis[b], P. Thuiner[b], Y. Tsipolitis[f], S.E. Tzamarias[e], R. Veenhof[b], X. Wang[d], S. White[b,**], Z. Zhang[d], Y. Zhou[d]

[a]*IRFU, CEA, Université Paris-Saclay, F-91191 Gif-sur-Yvette, France*
[b]*European Organization for Nuclear Research (CERN), Geneve 1211, Switzerland*
[c]*Institue of Nuclear Physics, NCRS Demokritos, 15310 Aghia Paraskevi, Athens, Greece*
[d]*University of Science and Technology of China, 96 JinZhai Road, Hefei, China*
[e]*Department of Physics, Aristotle University of Thessaloniki, Thessaloniki, Greece*
[f]*National Technical University of Athens, Athens, Greece*
[g]*Laboratório de Instrumentação e Física Experimental de Partículas, Lisbon, Portugal*

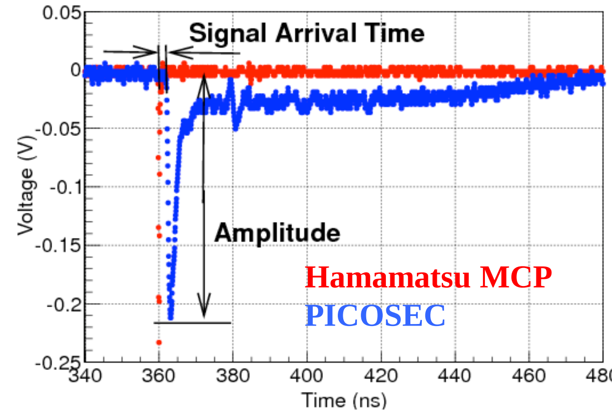

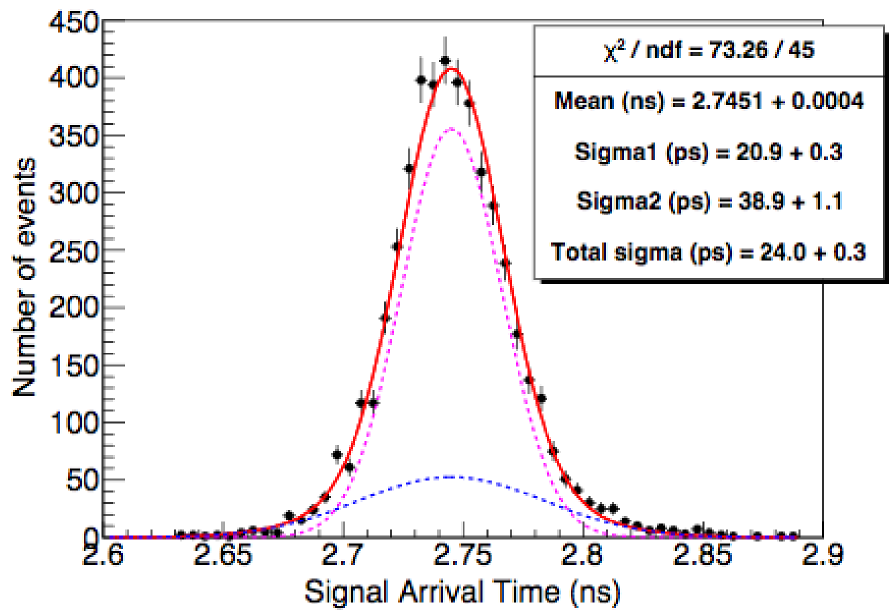

Figure 12: Beam test: An example of the signal arrival time distribution for 150 GeV muons, and the superimposed fit with a two Gaussian function (red line for the combination and dashed blue and magenta lines for each Gaussian function), for an anode and drift voltage of 275 V and 475 V, respectively. Statistical uncertainties are shown.

The Goals

- Suppress primary ionization by reducing the drift gap (200 nm)
  - ✓ Limit diffusion
  - ✓ Pre-amplification possible

- Use a Cerenkov radiator
  - ✓ Photoelectrons emitted at the cathode (fixed distance from the mesh)

Pre-amplification will
➔ reduce the effect of longitudinal diffusion
➔ limit contribution of gas ionization

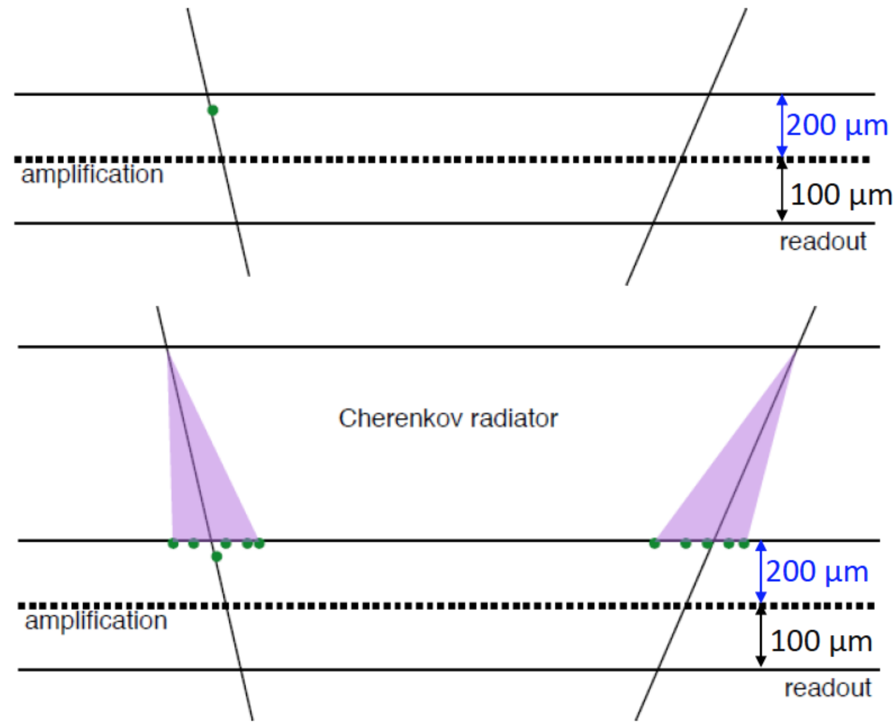

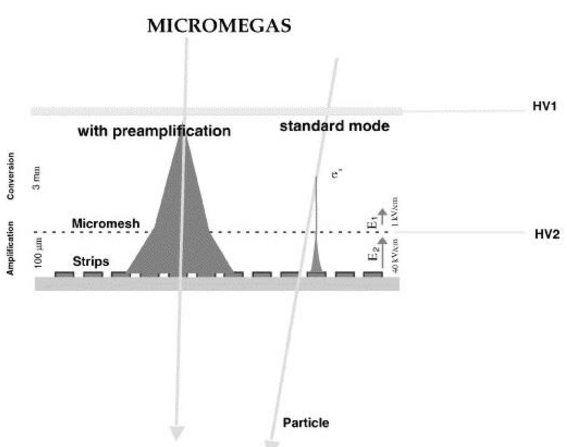

PICOSEC: Charged particle timing to 24 picosecond precision with a Micromegas based detector

J. Bortfeldt[b], F. Brunbauer[b], C. David[b], D. Desforge[a], G. Fanourakis[c], J. Franchi[b], M. Gallinaro[g], I. Giomataris[a], T. Gustavsson[a], C. Guyot[a], F.J. Iguaz[a,*], M. Kebbiri[a], P. Legou[a], J. Liu[d], M. Lupberger[b], O. Maillard[a], I. Manthos[e], H. Müller[b], V. Niaouris[e], E. Oliveri[b], T. Papaevangelou[a], K. Paraschou[e], M. Pomorski[a], B. Qi[d], F. Resnati[b], L. Ropelewski[b], D. Sampsonidis[e], T. Schneider[b], P. Schwemling[a], L. Sohl[b], M. van Stenis[b], P. Thuiner[b], Y. Tsipolitis[f], S.E. Tzamarias[e], R. Veenhof[b], X. Wang[d], S. White[b,**], Z. Zhang[d], Y. Zhou[d]

[a]*IRFU, CEA, Université Paris-Saclay, F-91191 Gif-sur-Yvette, France*
[b]*European Organization for Nuclear Research (CERN), Geneve 1211, Switzerland*
[c]*Institue of Nuclear Physics, NCRS Demokritos, 15310 Aghia Paraskevi, Athens, Greece*
[d]*University of Science and Technology of China, 96 JinZhai Road, Hefei, China*
[e]*Department of Physics, Aristotle University of Thessaloniki, Thessaloniki, Greece*
[f]*National Technical University of Athens, Athens, Greece*
[g]*Laboratório de Instrumentação e Física Experimental de Partículas, Lisbon, Portugal*

Single-anode prototype

Tests with UV lamp / laser ➔ quartz windows

Sensor:

Microbulk Micromegas ø 1cm
- Possibility to deposit CsI on the mesh surface
- Capacity ~ 35 pF

Bulk Micromegas ø 1cm
- Capacity ~ 8 pF
- Amplification gap 64 / 128 / 192 μm

Thin-mesh Bulk Micromegas (~5 μm)
- High optical transparency
- Amplification gap 128 μm

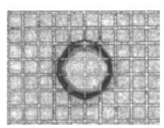

☞ Ensure homogeneous small drift gap & photocathode polarization

Photocathodes: MgF2 crystal +
- Metallic substrate + CsI
- Metal (Cr, Al)
- Metallic substrate + polycrystalline diamond
- *Boron-doped diamond*

☞ New stainless steel chamber for sealed mode operation

Very thin detector active part (<5 mm)

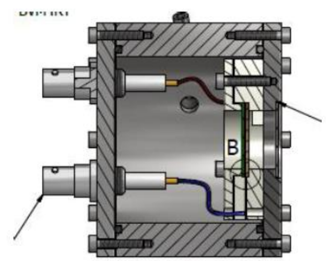

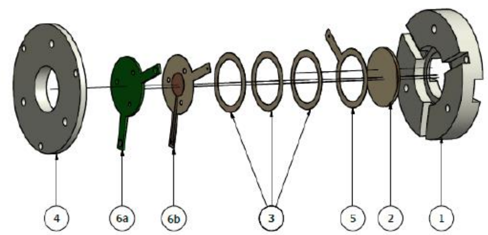

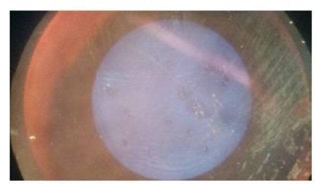

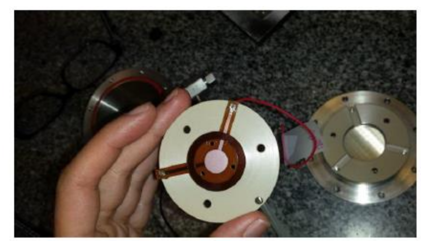

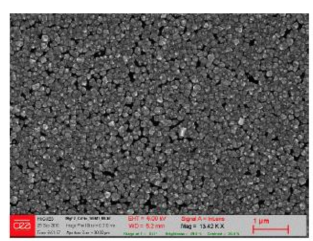

SPS measurement Setup

Triggering, Tracking and Timing

Tracker3 | 5mm hole VETO scintillator | 10cm x 10cm scintillator | MCP-PMT | Tracker2 | 5mm x 5mm scintillator | 5mm x 5mm scintillator | Tracker1

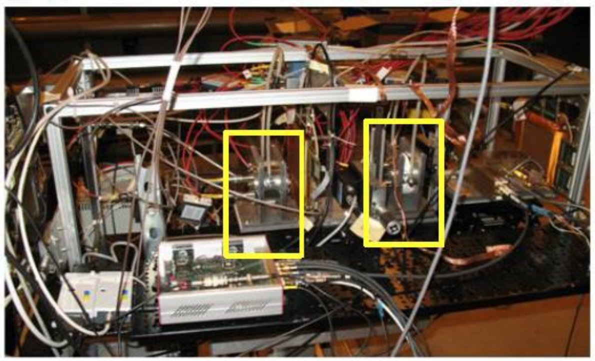

DAQ

SAMPIC

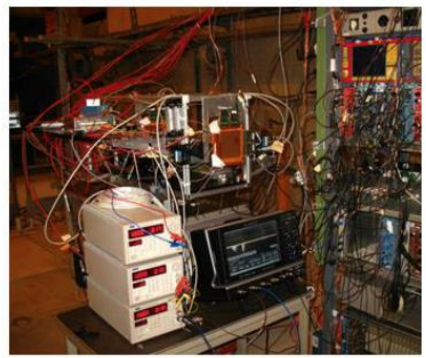

Oscilloscope

SRS

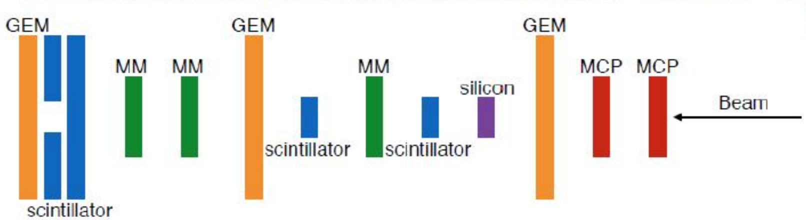

- Trigger: coincidence of two 5x5 mm2 scintillators and a veto downstream (avoid showers)
- Tracker: three GEMs to measure where the triggered particle passed (reject showers too)
- Time reference: two Hamamatsu MCP-PMTs (160 ps rise time)
- Tracking acquisition: APV25 + SRS
- Timing acquisition: CIVIDEC C2 preamp + 2x 2.5 GHz LeCroy scopes (synchronised with the tracker) and SAMPIC

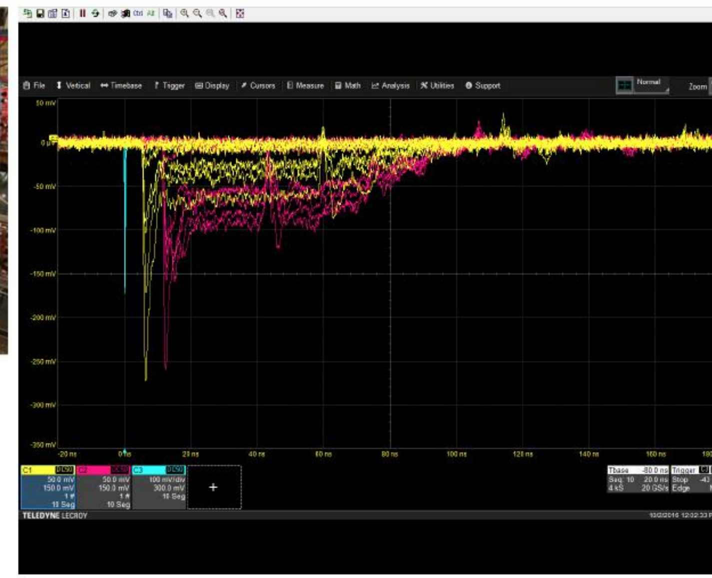

Signal Formation

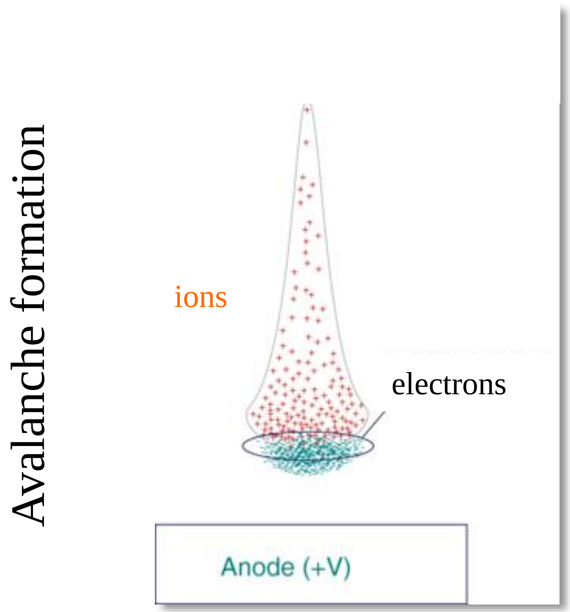

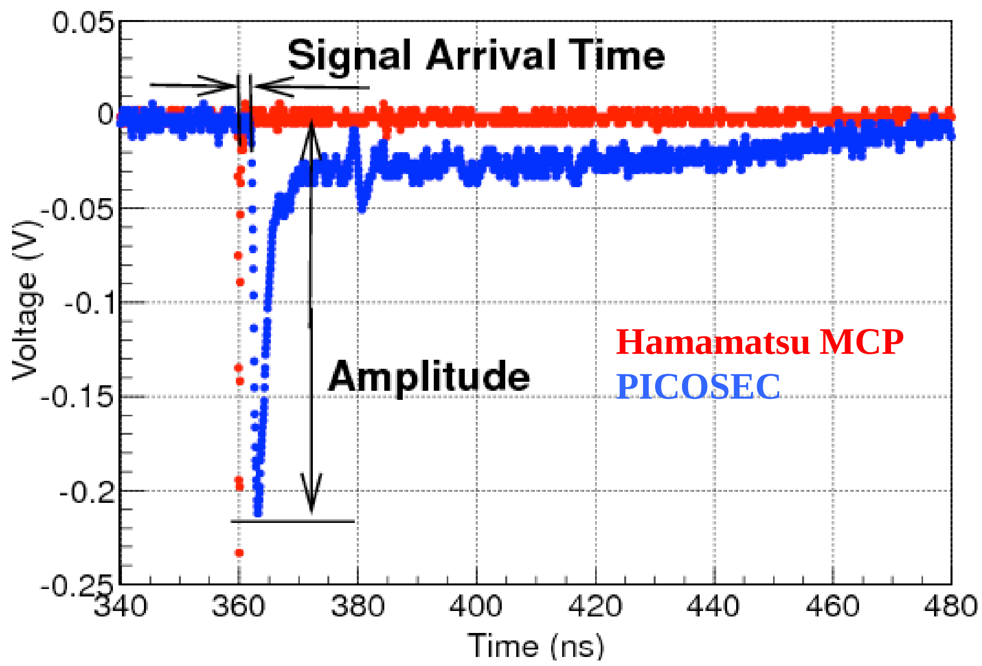

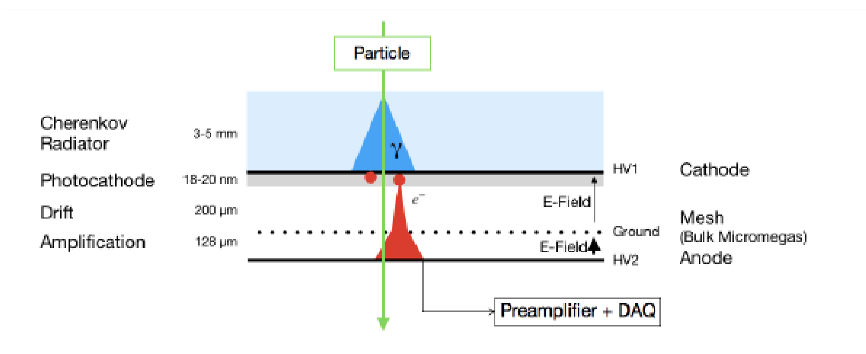

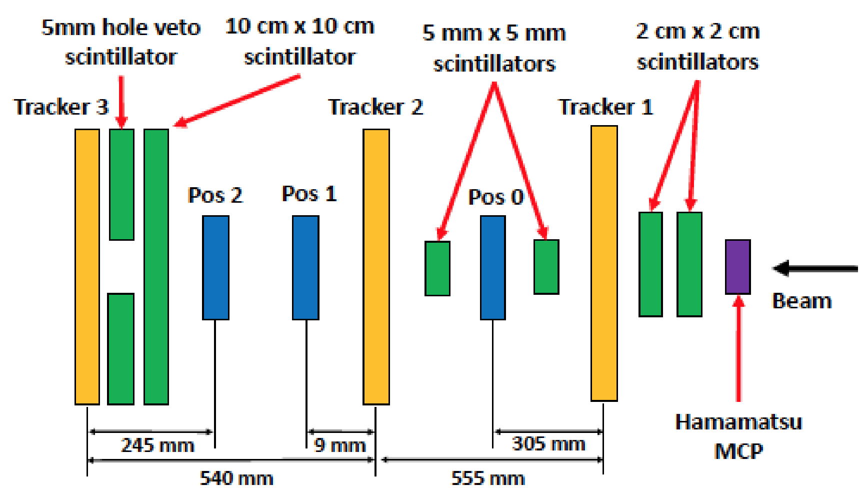

Timing Characteristics: Answers to many "Why" and "How"

- Development of experimental and data analysis strategies
- Employ precise simulation and development of phenomenological models
- Study and understand the interplay between competitive processes
- Optimize the detector's operational parameters

RD51 Open Lectures and Mini Week

11 Dec 2017, 12:00 → 15 Dec 2017, 18:30 Europe/Zurich

593-R-010 - Salle 11 (CERN)

Eraldo Oliveri (CERN), Spyros Tzamarias (Aristotle University of Thessaloniki (GR))

Description *Monday 11th December, 14:00 - Wednesday 13th December 12:30*

RD51 Open Lectures: Signal generation, modelling and processing

W. Riegler, R. Veenhof, F. Resnati, S. Tzamarias

Purpose of the lectures is to discuss new developments on the methods and tools used to describe the signal generating processes as well as techniques of analysing data of gaseous detectors. The lectures are geared towards people who are doing, or intend to do, research and developments on gas-based detectors but are also open to anyone interested on the subject.

Please, fill the registration to the Open Lectures (right panel) in particular if you are planning to follow them in person at CERN.

Lectures will be broadcasted via Vydio.

Access to the lectures is free. Certificate of Attendance will be provided under request.

see https://indico.cern.ch/event/676702/timetable/
and https://arxiv.org/abs/1712.05256

Recognize the "start" and "end" of the e-peak, as well as the "end" of the ion tail

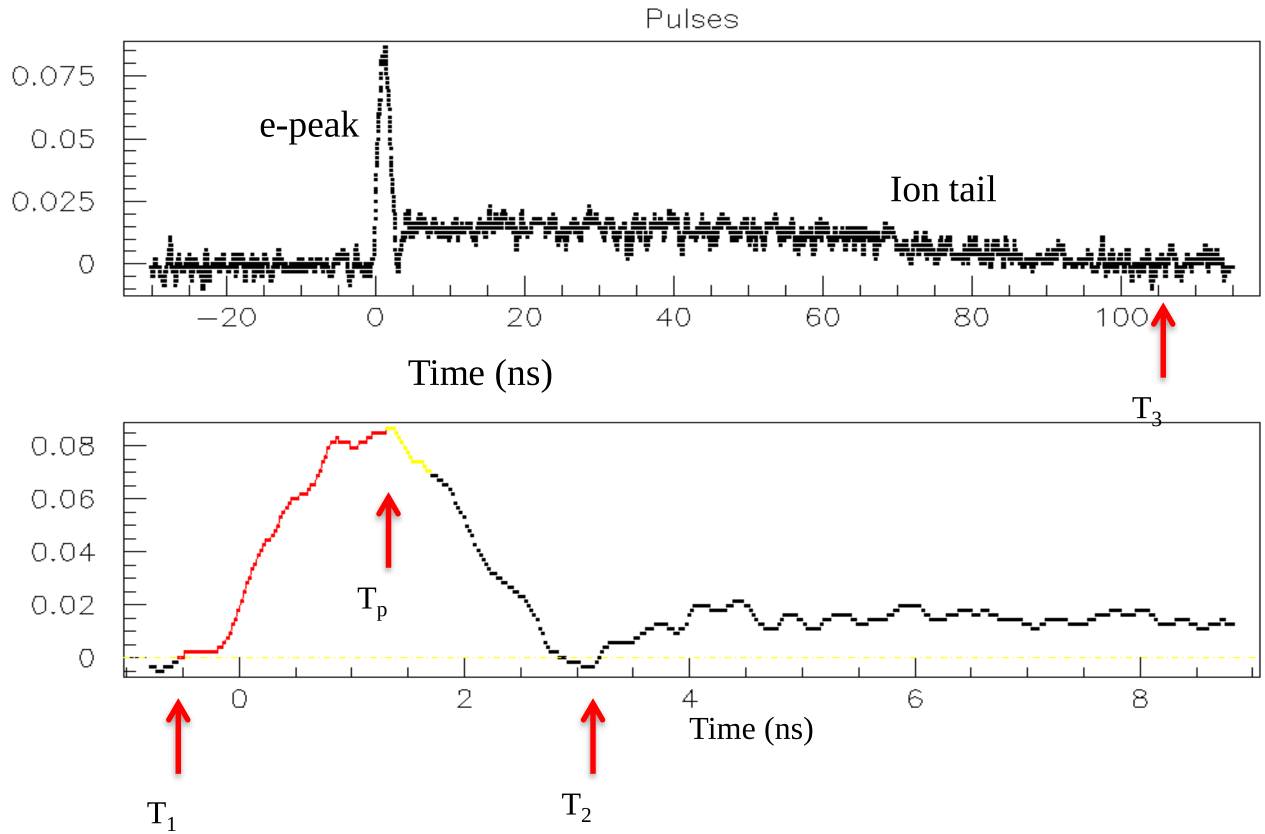

Evaluate charge by integrating the relevant part of the waveform

Definition of the e-peak Arrival Time
Fit the e-peak Leading Edge

Fit the e-peak leading edge in order to neutralize noise effects.
Several Functions have been used in the fits, including quadratic and cubic polynomials as well as logistic and generalized logistic functions

$$\frac{P_0}{1+\exp[-P_2(x-P_1)]}+P_3 \quad , \quad \frac{P_0}{\left(1+\exp[-P_2(x-P_1)]\right)^{P_3}}$$

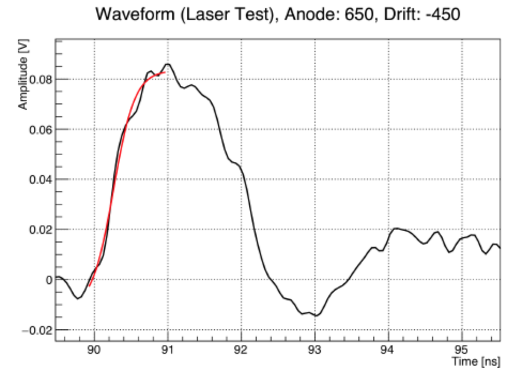

A fit of the whole e-peak was also tried using the difference of two logistic functions

$$f(t;p_0,p_1,p_2,p_3,p_4,p_5,p_6)=\frac{p_0}{\left(1+e^{-(t-p_1)p_2}\right)^{p_3}}-\frac{p_0}{\left(1+e^{-(t-p_4)p_5}\right)^{p_6}}$$

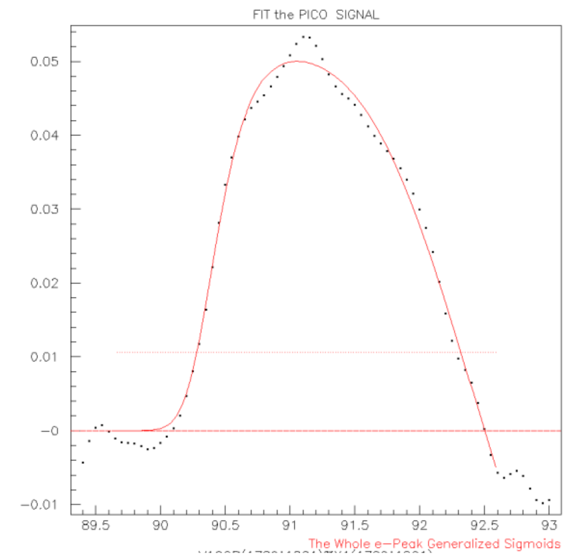

The results of these fit is also used to define the “start” and ”end” points of the e-peak waveform, to estimate charge and it is also used for timing

Define the e-peak arrival time at a Constant Fraction of the peak maximum

CFD Timing minimizes "slewing effects"

CFD Timing of raw pulses suffers from noise

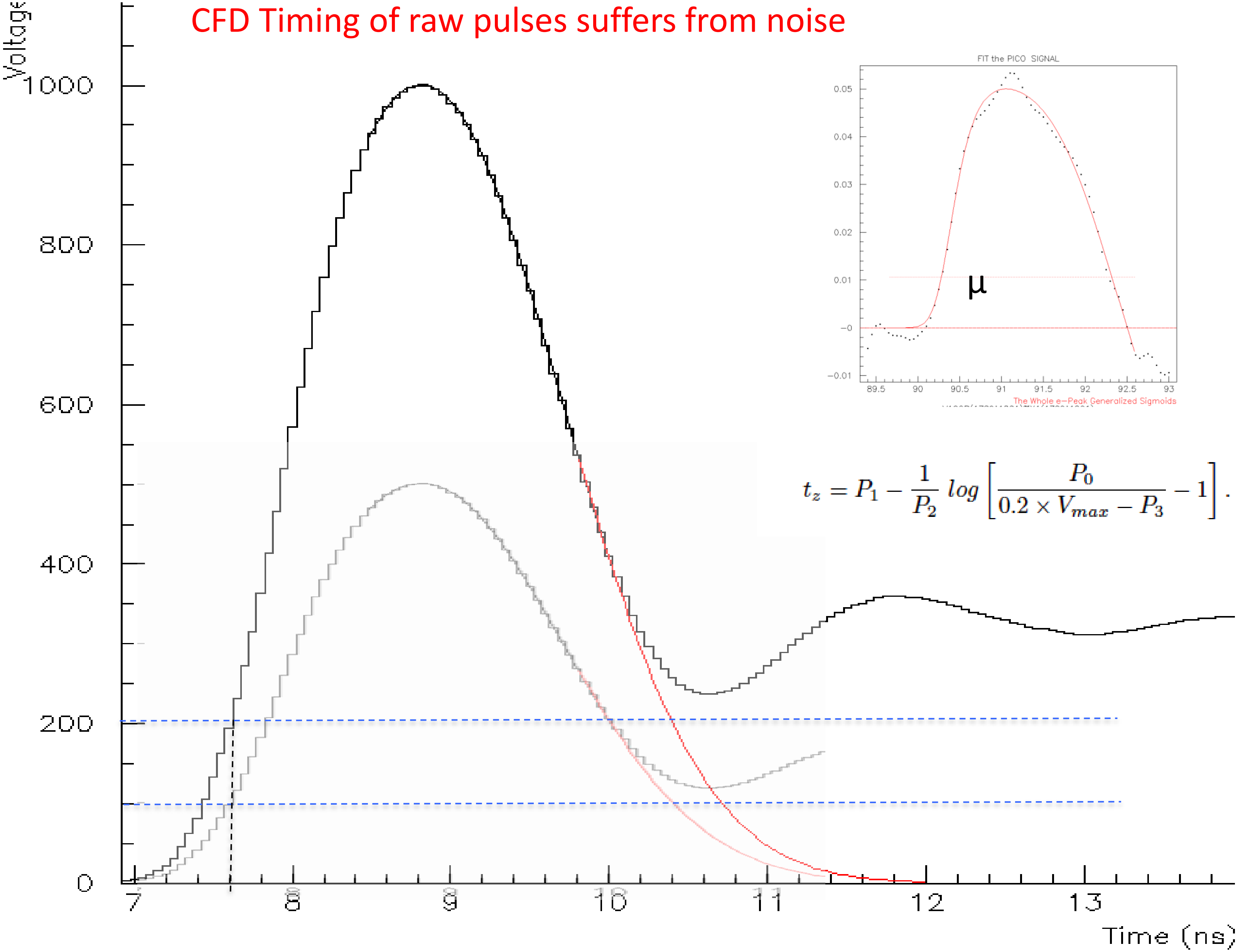

$$t_z = P_1 - \frac{1}{P_2}\, log\left[\frac{P_0}{0.2 \times V_{max} - P_3} - 1\right].$$

Fitting the e-peak waveform helps to estimate the charge in “impossible” cases

Example: small pulses

Define the start and the end of the e-peak

Estimate the charge

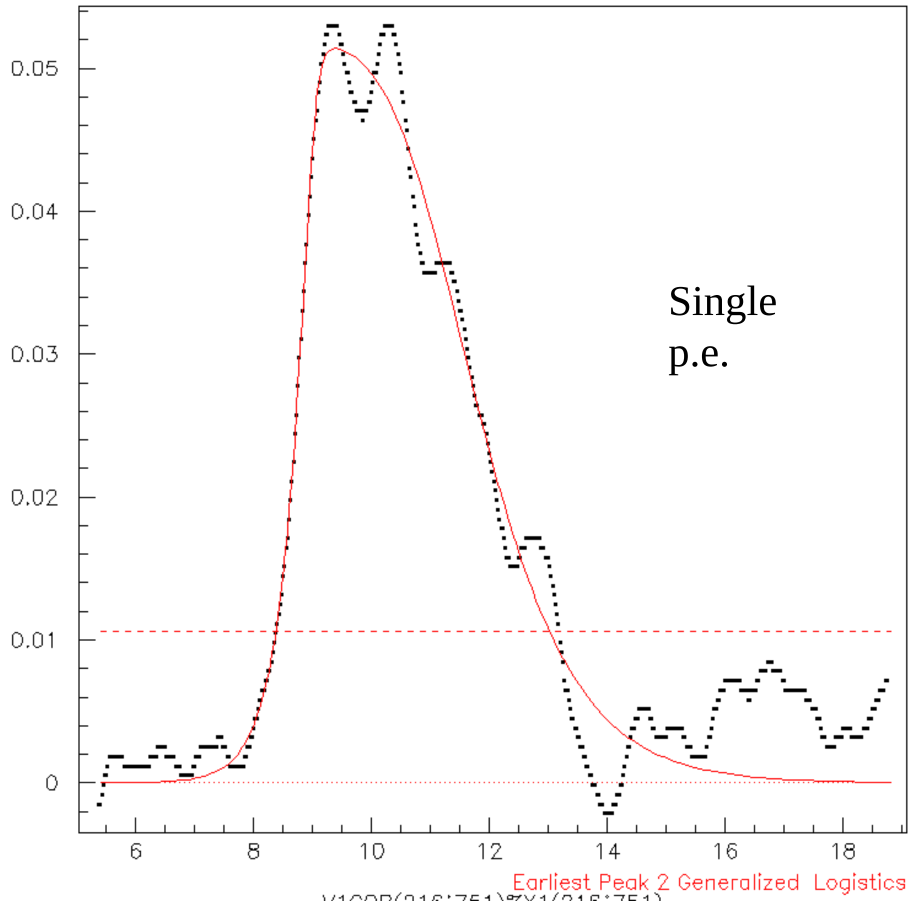

Why not using filtering algorithms???

Is it possible to filter-out the noise ?

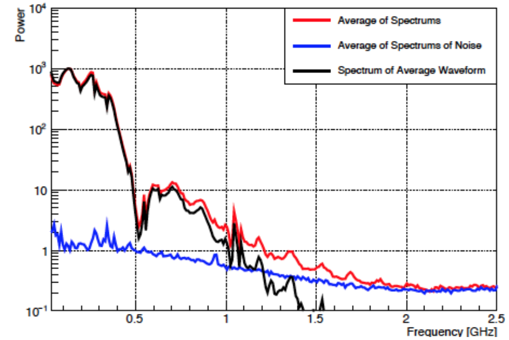

An example of filtering out the noise
(cut at 1.5 GHz)

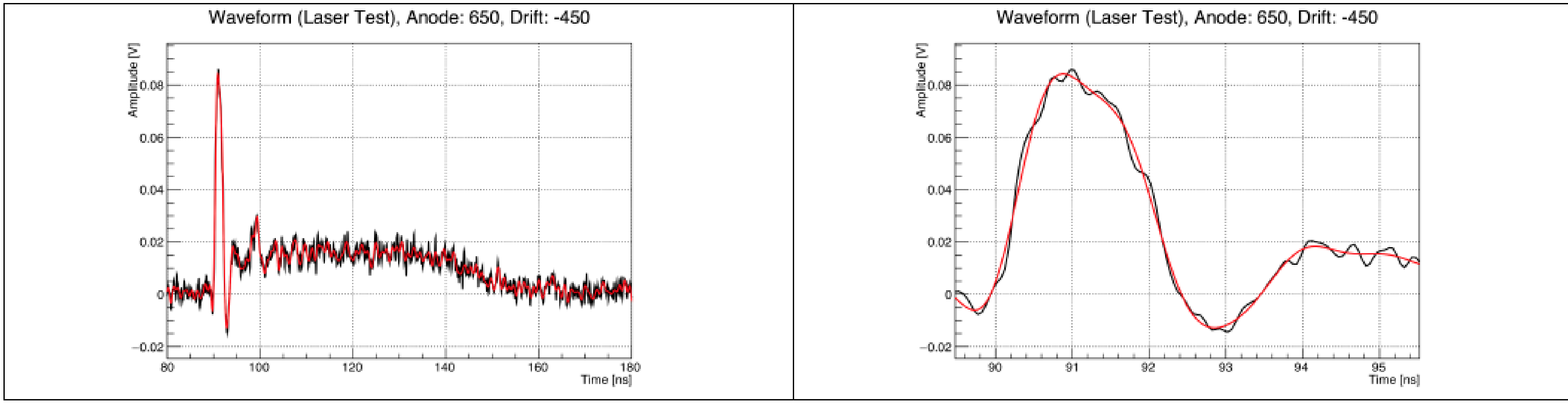

In these examples (PICOSEC-MicroMegas), the use of filtering before fitting the leading edge of the pulse DOES NOT improve the timing resolution, i.e. a conservative frequency cut does not improve the timing resolution and a strong frequency cut deforms the rising edge of the pulse worsening the time resolution
(see V. Niaouris Talk)

Back to the results

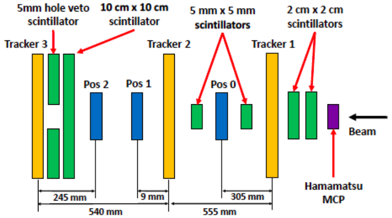

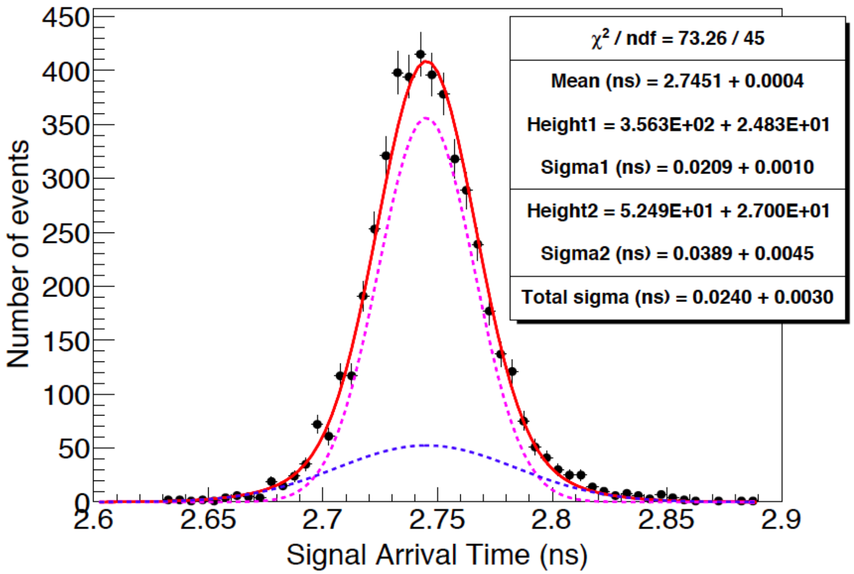

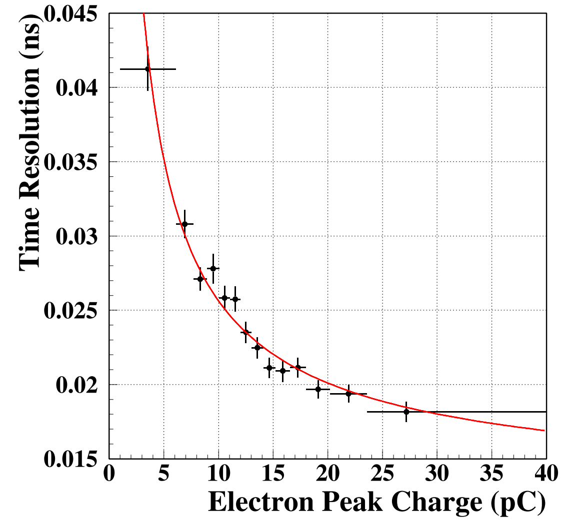

- **Why the Δt distribution is not Gaussian ?**
- **Why the Resolution depends on the e-peak size?**

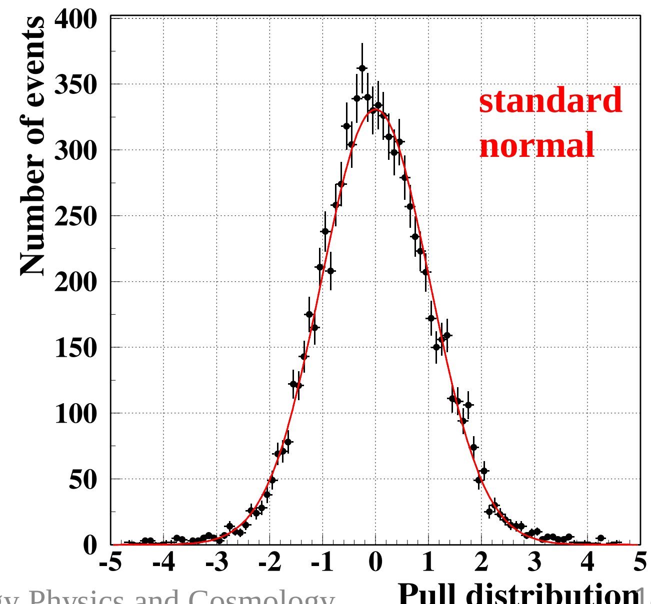

Back to basics

•The Cherenkov photons, produced when a relativistic muon (MIP) passes through the MgF_2 radiator, extract (per average) 10-11 photoelectrons from the CsI photocathode.

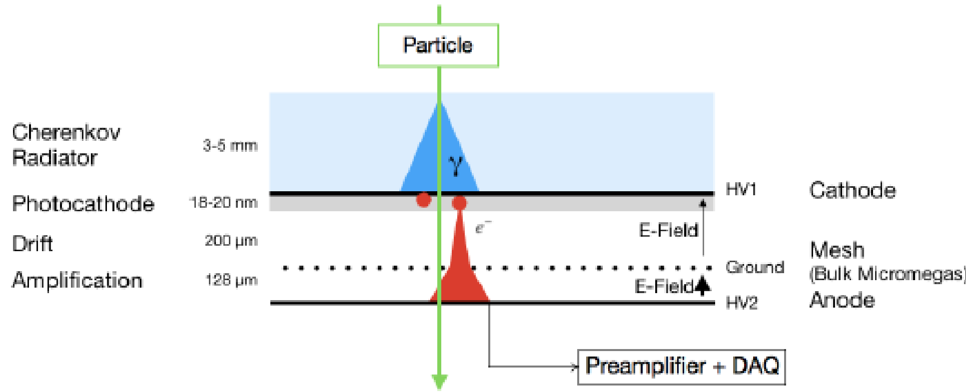

•The PICOSEC response to a MIP is the linear sum of its response to each of the produced (mutually uncorrelated) photoelectrons

•In order to understand the signal formation dynamics we studied the PICOSEC response to single photons, using a monochromatic laser beam

"Compass gas" ($Ne+10\%C_2H_6+10\%CF_4$) at 1 bar.

$CF_4+20\%C_2H_6$ at 0.5 bar

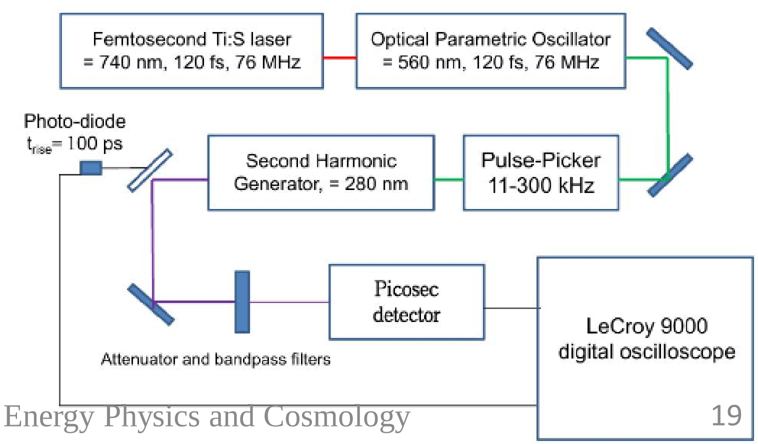

Does the “Polya” shape describe the e-peak charge and amplitude distributions?

Laser beam tests

Use data sets collected without any threshold on the picosec-MM signal to test the “Polya Hypothesis”

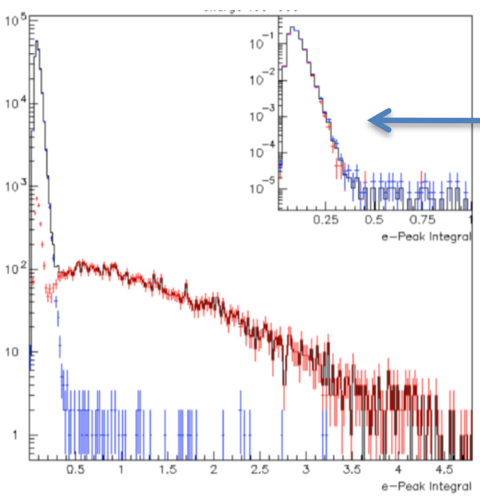

Use out-of-time events to model the noise

$$F\left(Q;C,\theta,\bar{Q}_e\right)=\frac{C}{Q_e}\frac{(\theta+1)^{(\theta+1)}\left(Q/\bar{Q}_e\right)^{\theta}}{\Gamma(\theta+1)}e^{-(\theta+1)Q/\bar{Q}_e}$$

Fit the charge spectrum produced by a single photoelectron

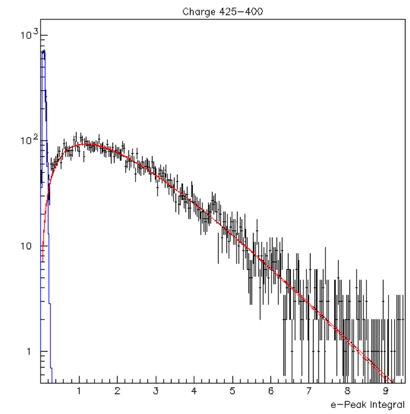

$$G\left(Q;C_1,C_2,\cdots C_k,RMS_e,<Q_e>\right)=\sum_{N=1}^{k}\frac{C_N}{\bar{Q}_e}\frac{(\theta+1)^{N(\theta+1)}\left(Q/\bar{Q}_e\right)^{N(\theta+1)-1}}{\Gamma\left(N(\theta+1)\right)}e^{-(\theta+1)Q/\bar{Q}_e}$$

$$number\ of\ events=\sum_{N=1}^{k}C_N$$

Fit the charge spectrum produced by several photoelectrons

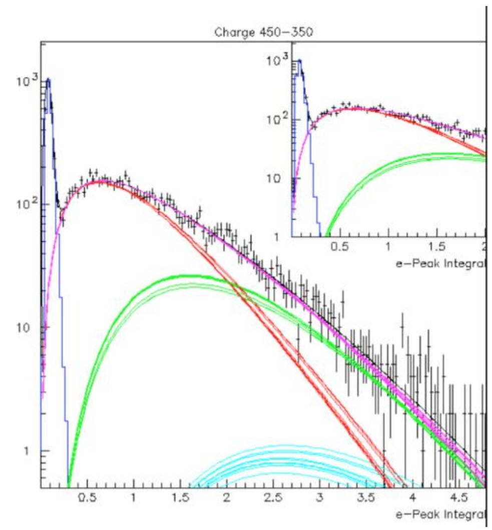

The Signal Arrival Time Depends on the size (Charge) of the e-peak

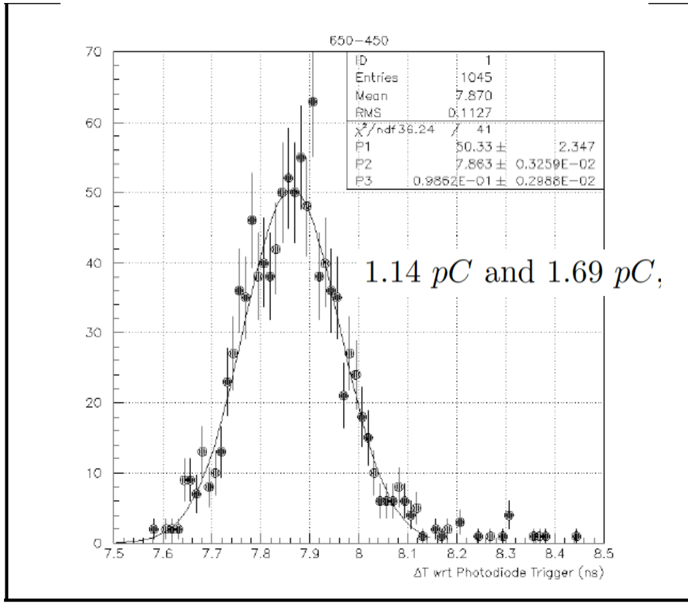

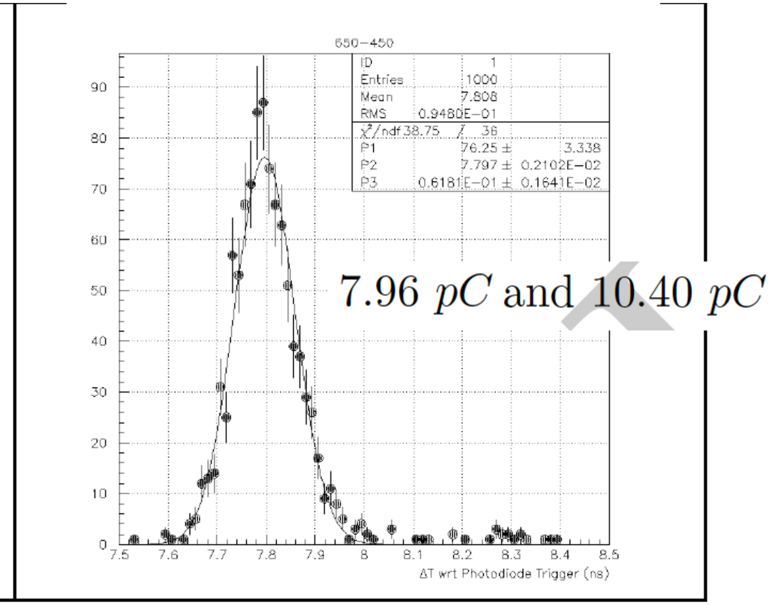

$$f(x) = \frac{b}{x^w} + a$$

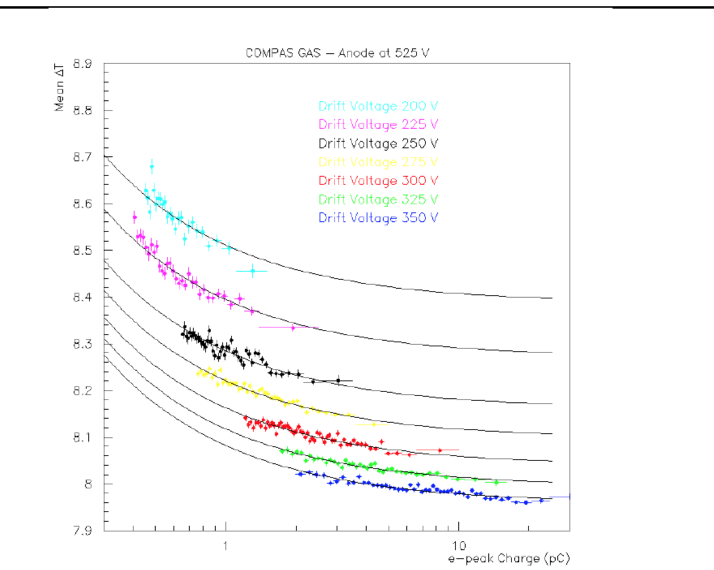

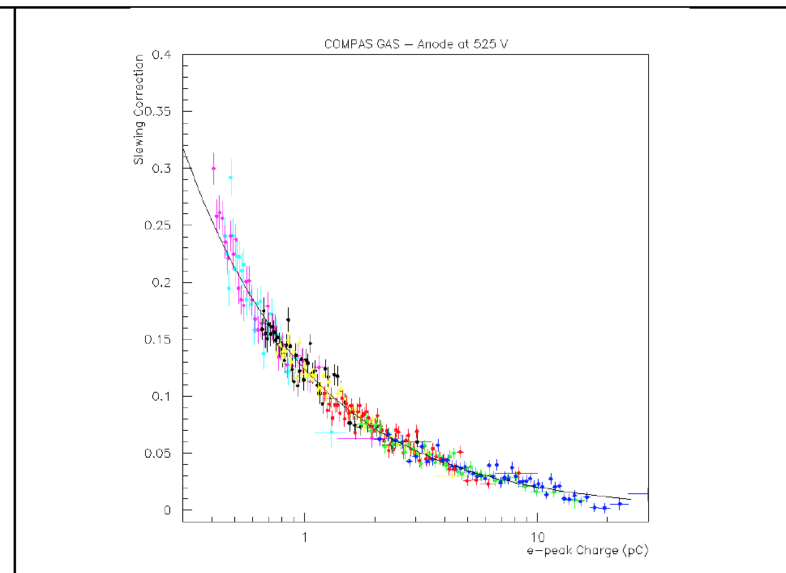

The Resolution depends on the size (Charge) of the e-peak

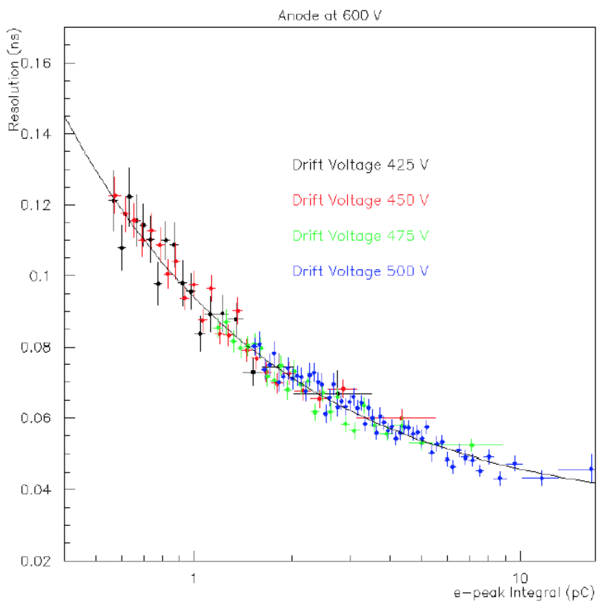

$$f(x) = \frac{b}{x^w} + a$$

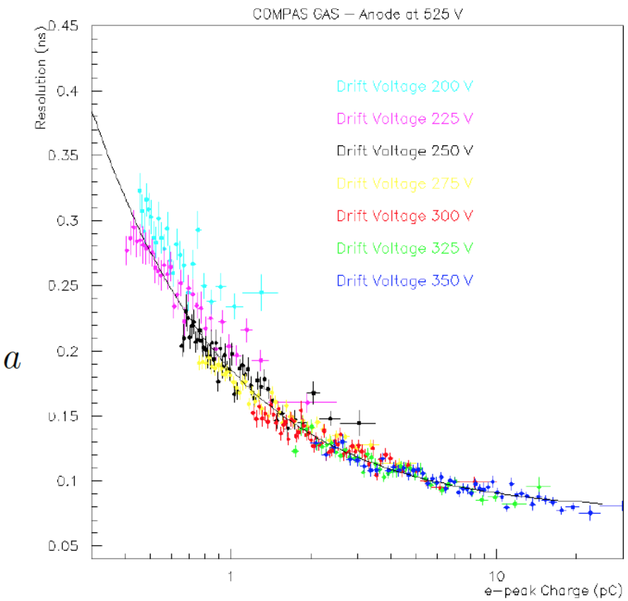

The SAT and Resolution dependence on the e-peak size, for constant anode field, follow the Same functional form independently of the applied anode field !!!!

The anode field does not alter significantly the SAT and Resolution dependence on the e-peak size. The anode field does not affects the timing characteristics !!!

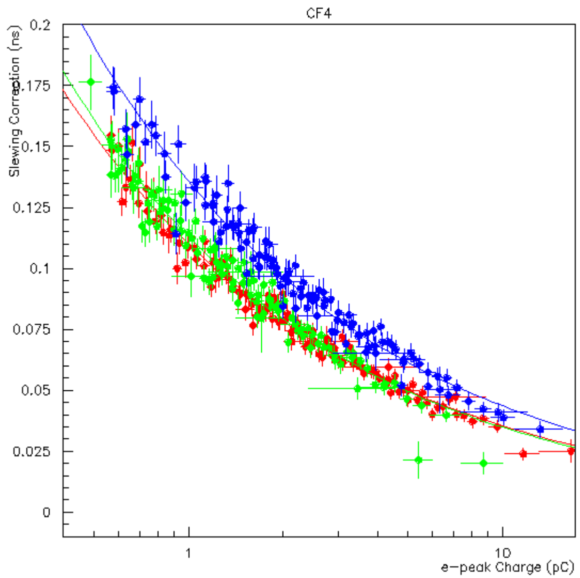

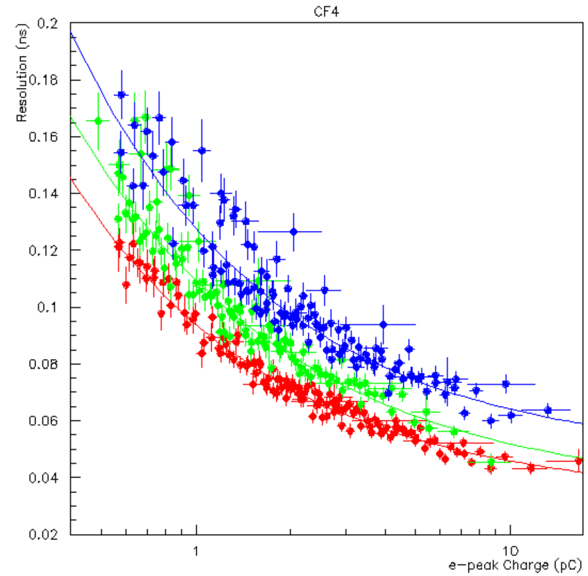

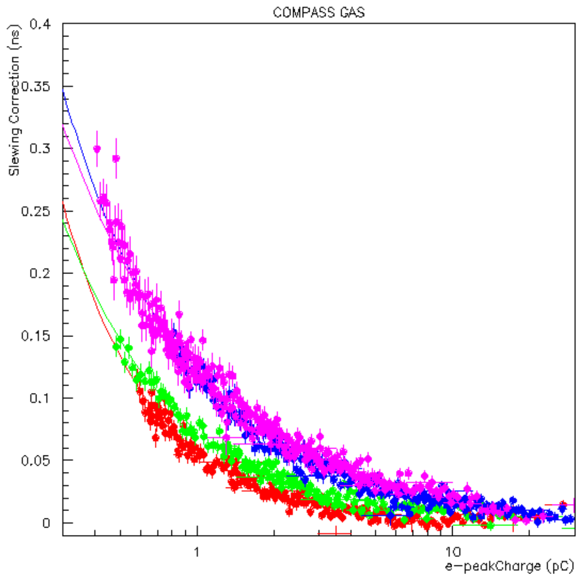

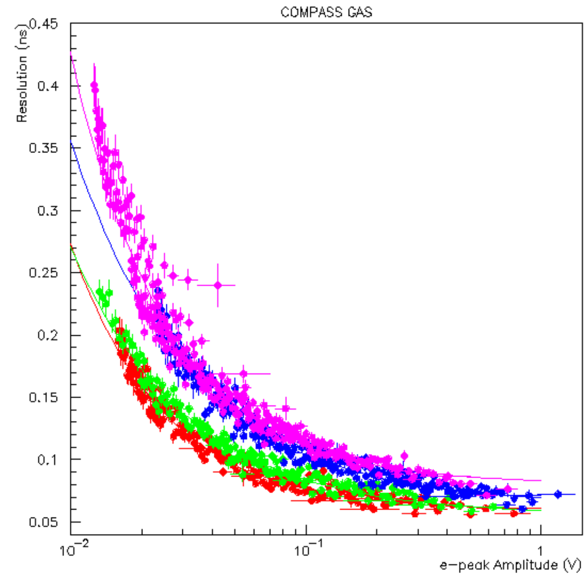

Counter-Intuitive: The Resolution dependence on the e-peak size is the same for all the drift fields (despite the different diffusion coefficients)

Counter-Intuitive: The SAT depends on the e-peak size. The dependence is the same for all the drift fields (within a constant delay due to the different drift velocities)

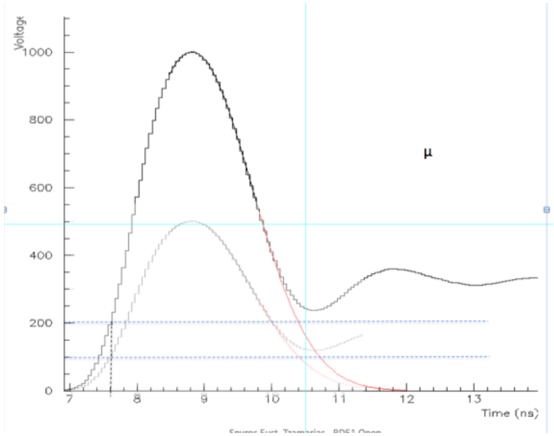

The CFD timing is slewing-free as long the pulse shape does not change with the pulse amplitude

The PICOSEC pulse shape remains almost constant. The waveform shifts because of some physical process !!!

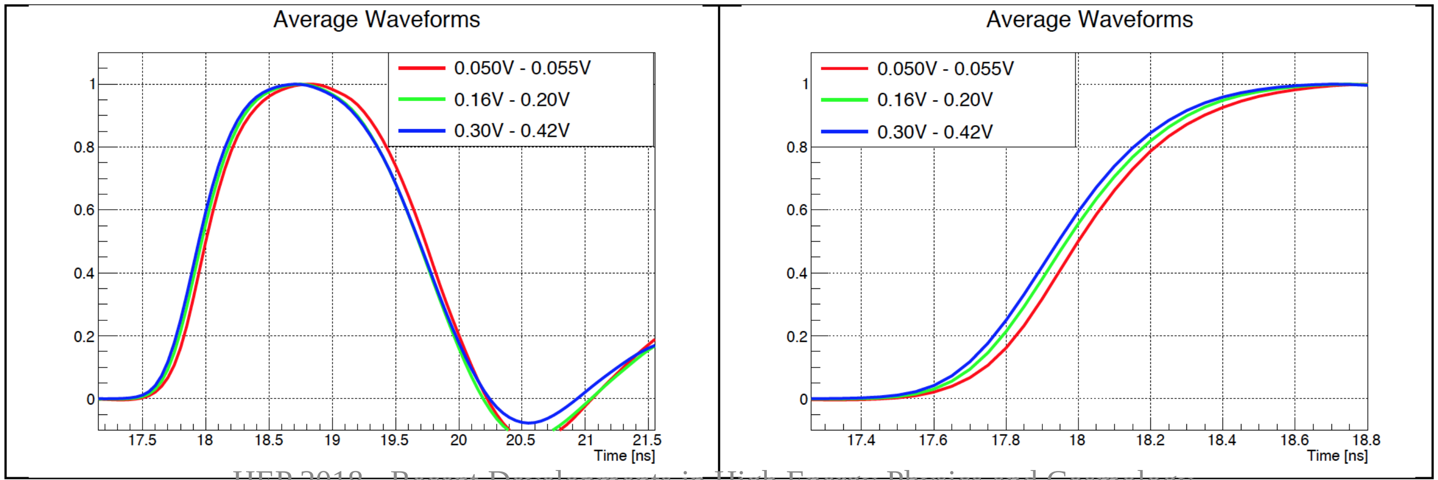

- **We should use a detail-simulation (including all the relevant atomic and molecular phenomena) to simulate the PICOSEC response to single photoelectrons**
- **Garfield++**
- **First Difficulty: Garfield++ simulates up to the induced current on the anode**
- **We should extract the electronics' response to the PICOSEC signal (couplings, preamps etc) from the data**

We have developed a statistical technique (proving that is consistent and unbiassed) which convolves Garfield++ predictions with a parameterization of the electronics' response and estimates the relevant parameters by fitting the average pulse shape observed in the data.

(see K. Paraschou talk and Master Thesis)

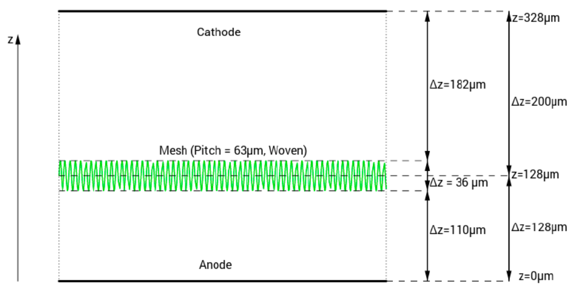

Figure 2.1: Diagram of the simulated detector model. The geometry is periodic in the plane that is perpendicular to the z-axis (electric field). The reference $z = 0$ is the anode.

Stage 1: Simulation of the pre-amplification region.

Stage 2: Simulation of the amplification region.

Stage 3: Combination of Stage 1. and Stage 2., and convolution with the parametrization of the electronics' response to generate waveforms.

$$f(t; p_0, p_1, p_2, p_3, p_4, p_5, p_6) = \frac{p_0}{(1 + e^{-(t-p_1)p_2})^{p_3}} - \frac{p_0}{(1 + e^{-(t-p_4)p_5})^{p_6}}$$

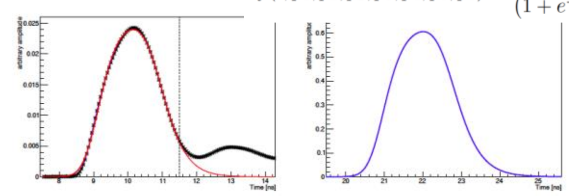

(a) (b)

Figure 2.7: (a) The black points in the right plot correspond to the experimental average waveform for events with an electron peak charge above 15. pC. This region was chosen to prevent the SAT dependence from affecting the result. The fit result is shown in the red line of the plot. The dashed line corresponds to the right limit of the fit region. (b) The final impulse response as a function of time is shown.

The shapes of the simulated pulses, for different drift voltages (same anode voltages) and for different e-peak sizes, agree very well with the data

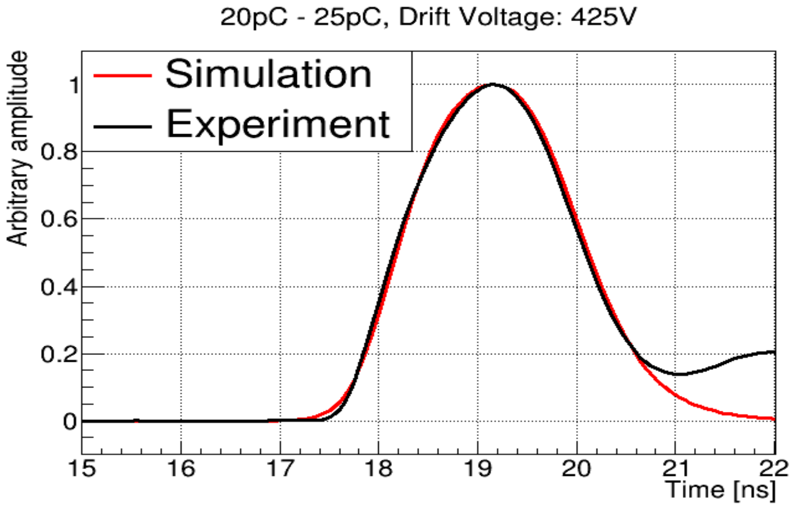

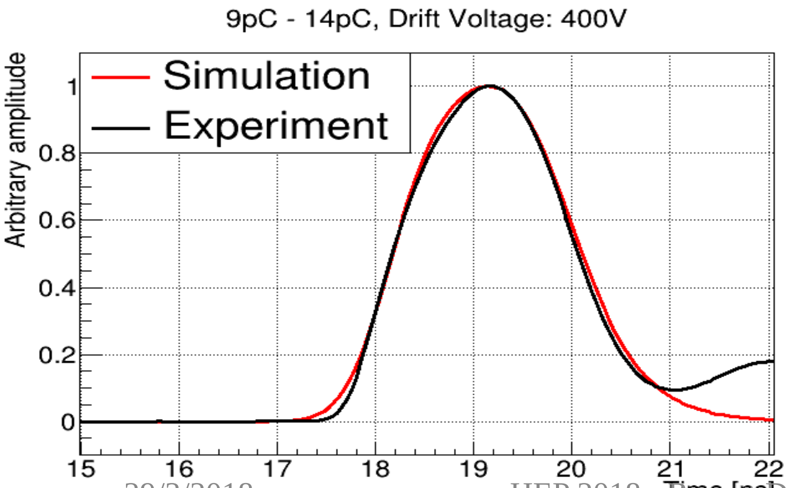

The worst case – perhaps due to noise/reflections contributions

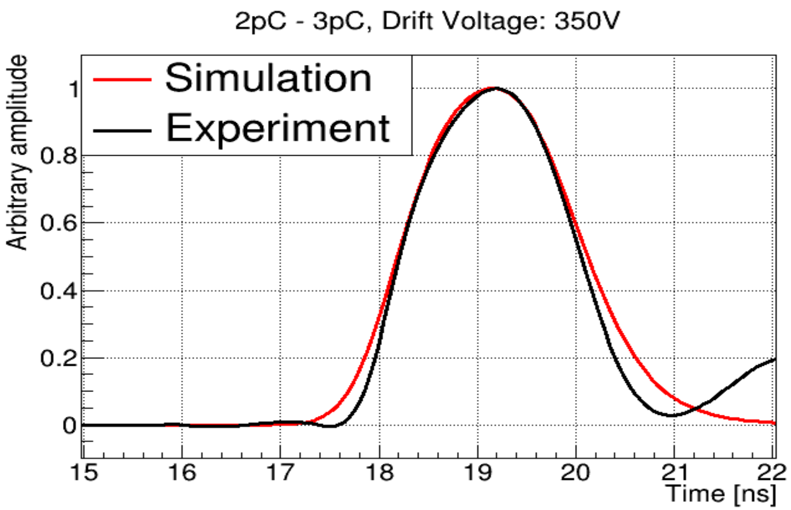

We have to scale the MC charge (or amplitude) predicted distributions in order to take into account the electronics' gains. We expected that by adjusting the scale factor at some drift operating voltage we should predict all the other distributions of events collected with the same anode but different drift voltages, WITHOUT any extra fine tuning.

However…

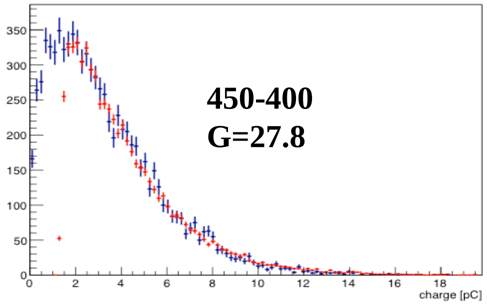

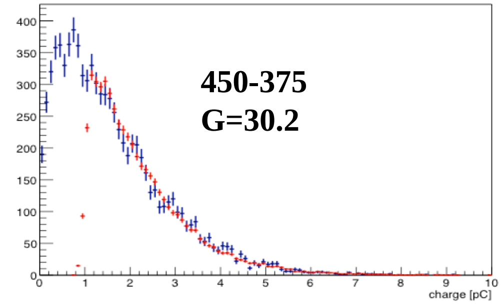

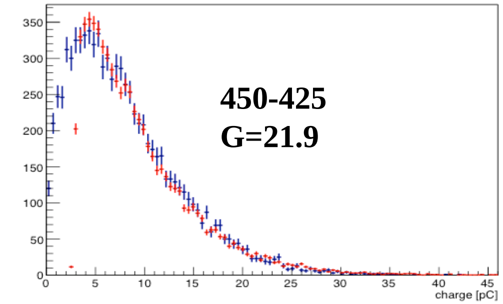

It is known that the COMPASS gas mixture has a significant penning effect. Until now this effect was ignored in the simulation. We consider different penning transfer rates to examine its behaviour.

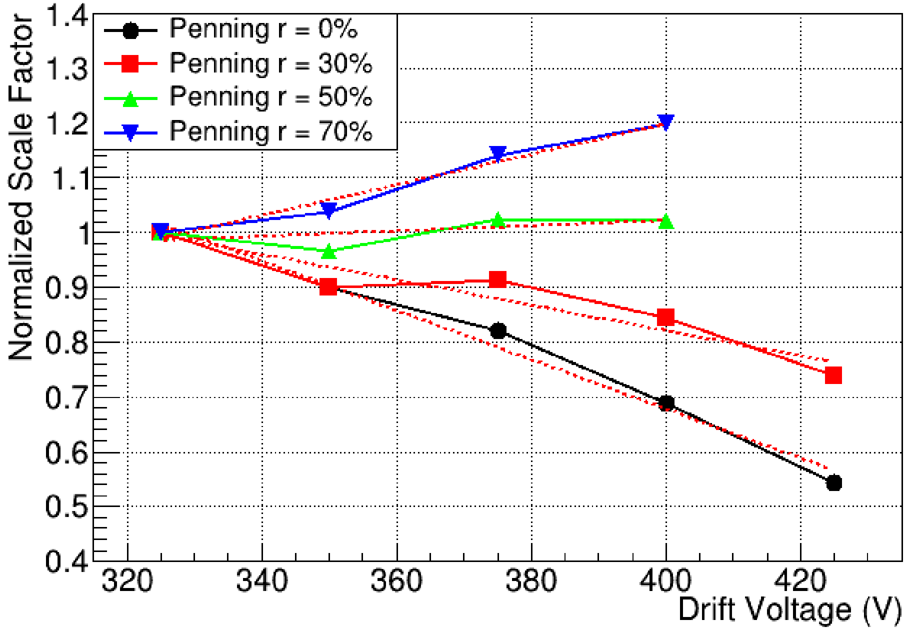

Approximately, for a transfer rate r ≈ 50%, the scale factor is not dependent on the drift voltage setting.

(see K. Paraschou talk)

Fig: Scale factor, G, as a function of drift voltage, divided by the scale factor at 325 V. Red lines dashed represent linear fits.

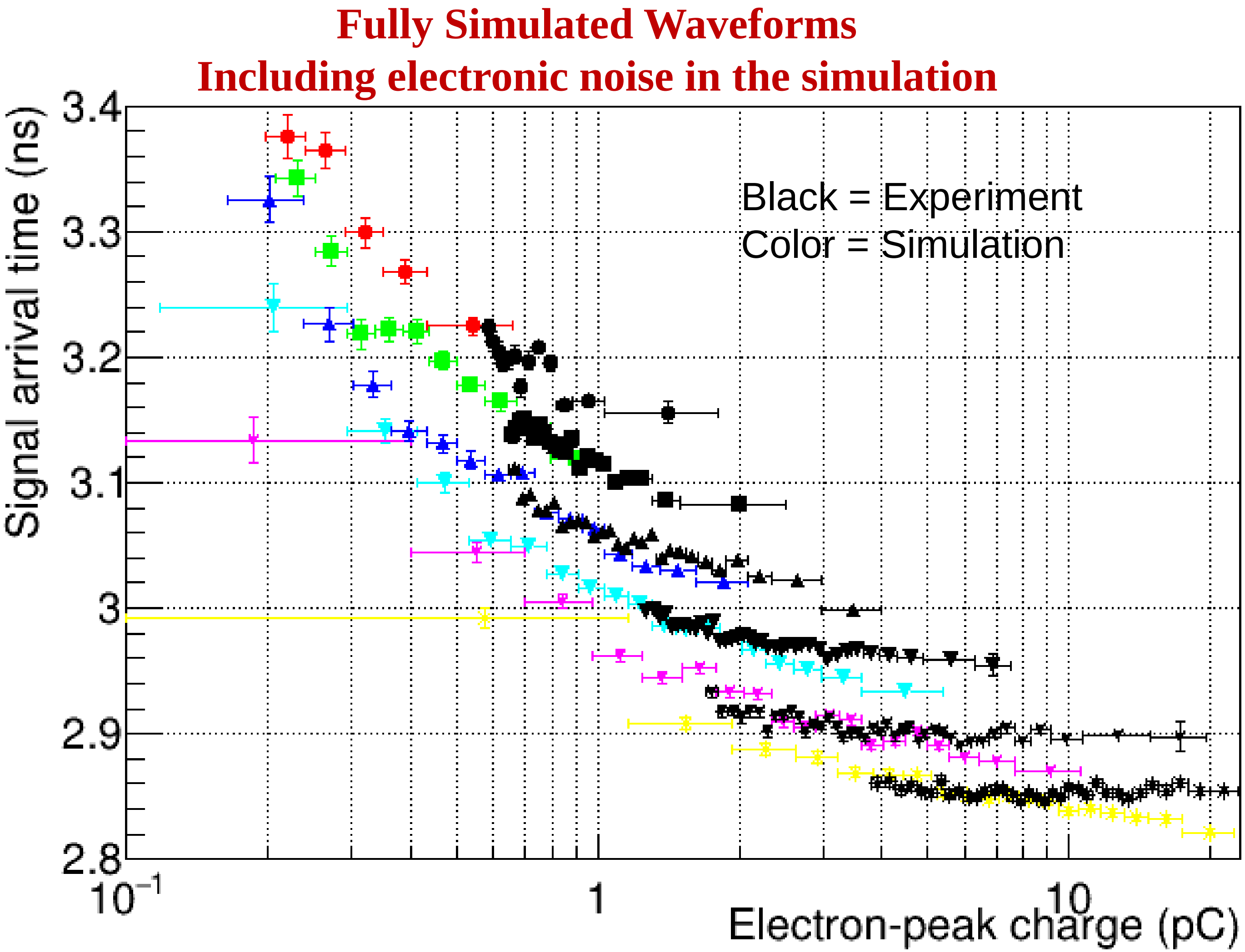

A simple 2.5mV RMS, uncorrelated noise inclusion makes the simulation's predictions to agree much better with the experiment.

Include electronic noise in the simulation

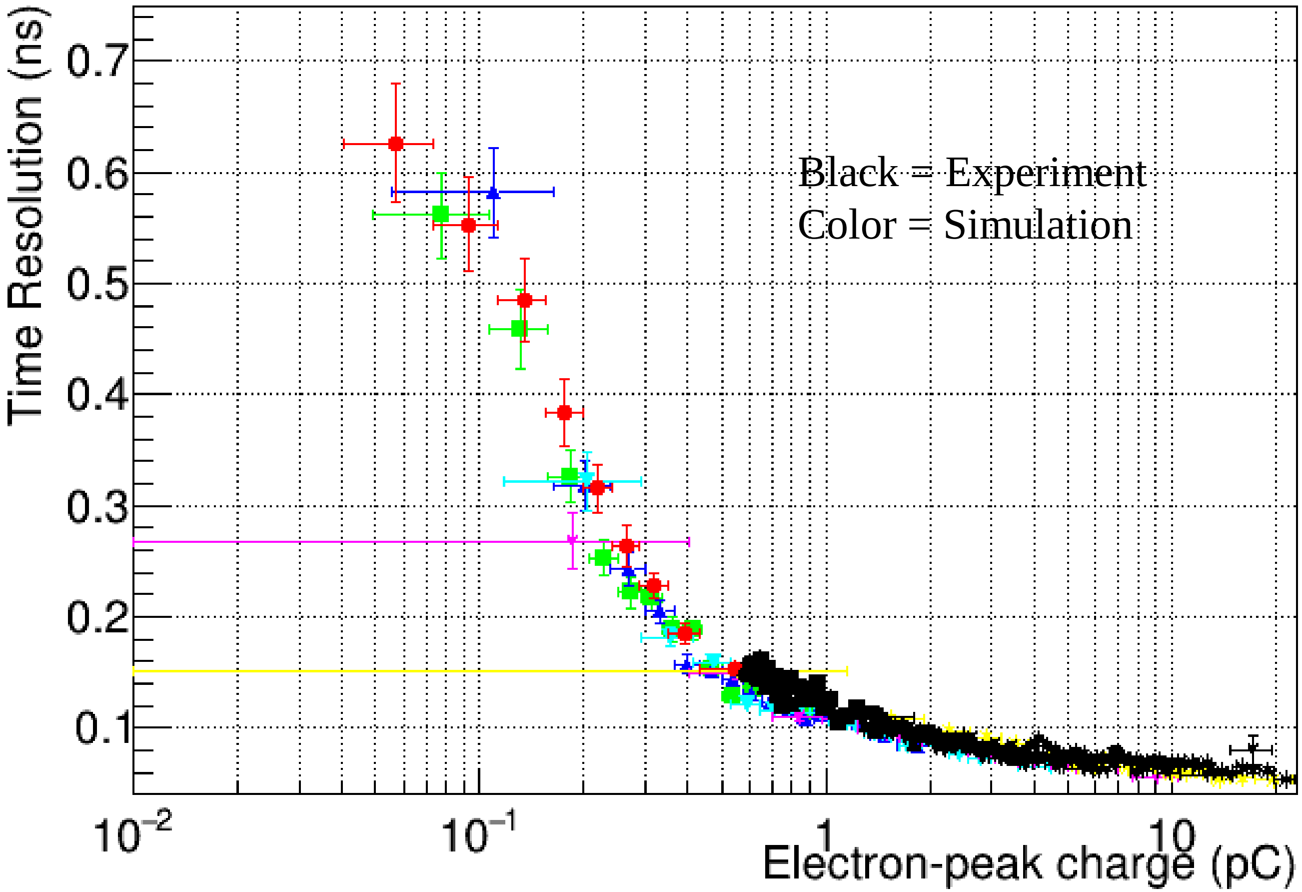

The simple 2.5mV RMS noise inclusion makes the simulation's resolution agree almost perfectly with the experiment.

Furthermore, the simulation predicts that large pulses are arriving earlier than smaller pulses whilst the pulse shape remains almost the same, as it has been observed in the data.

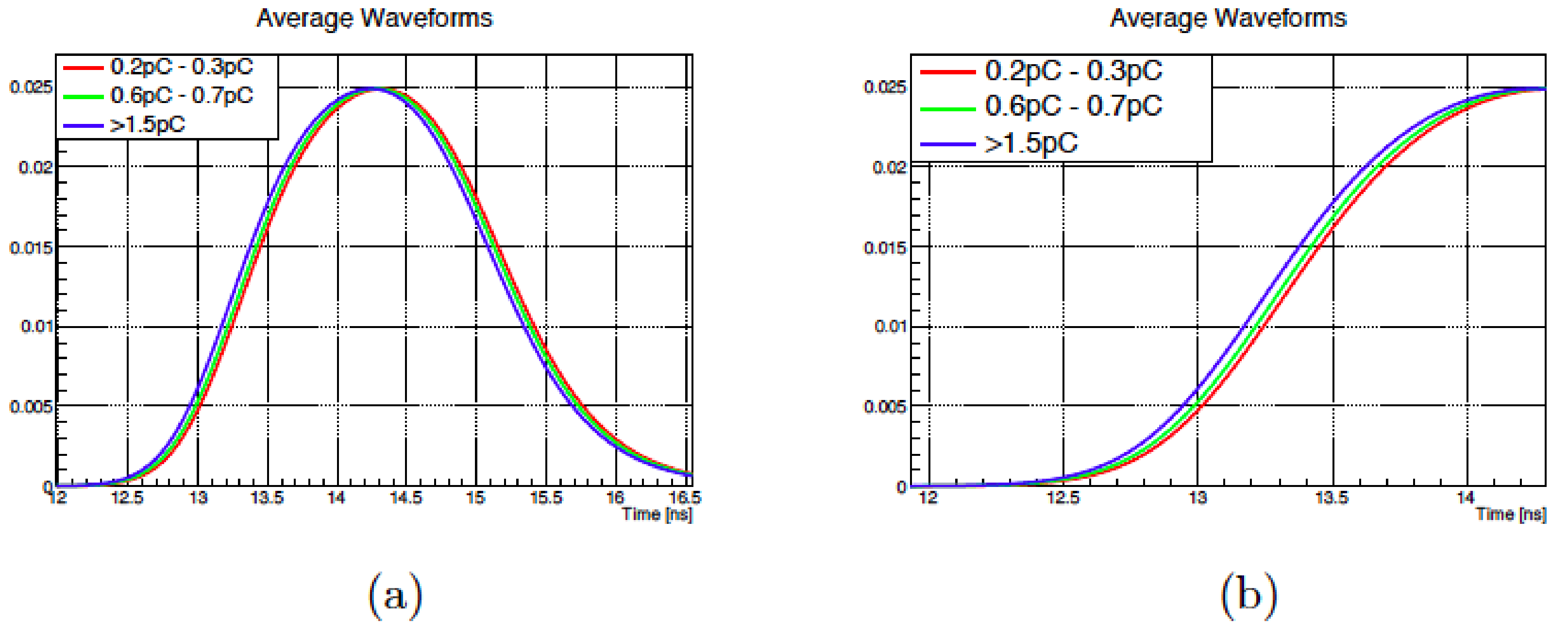

Figure 2.12: Both figures show the average simulated waveforms in different bins of electron peak charge, denoted by the color code. In (a), the whole electron peak is shown, whilst in (b) the focus is on the leading edge.

•Garfield++ includes all the relevant atomic and molecular processes. However, the fact that Garfield++ predictions (convolved with the electronics response) describe the PICOSEC timing characteristics does not enlighten us for their origin (e.g. why SAT depends on the e-peak size?)

•At this point Garfield++ is like a "black box"

In the following…

- Identify the main microscopic parameters that correspond to the macroscopic (experimental) observables: SAT and Resolution
- Identify the processes which are responsible for varying the main microscopic parameters
- Build a phenomenological model to describe the mechanisms of variation and compare with the Garfield++ predictions

(for details see K. Paraschou MSc Thesis and talk)

A single avalanche

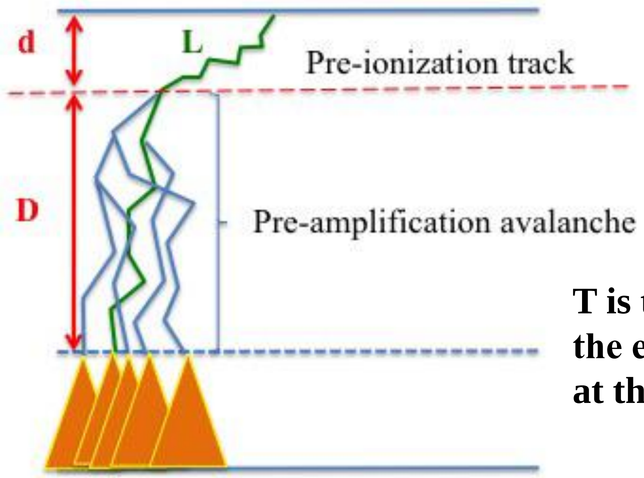

T is the mean value of all the electrons' arrival times at the mesh

Many avalanches with the same length D

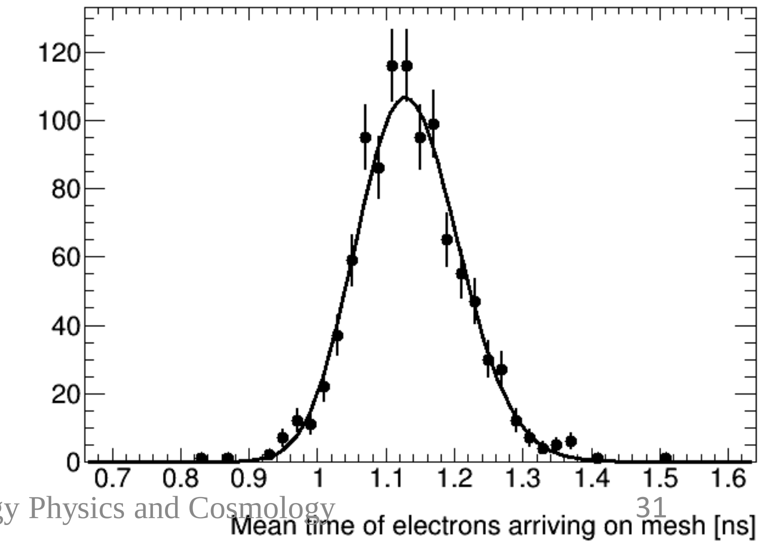

Select simulated waveforms with e-peak charge in a certain (narrow) region of Charge
Evaluate the experimental arrival Time of each waveform
Evaluate the corresponding T, i.e. the mean arrival time on the mesh of all the pre-amplification avalanche's electrons
Study the correlation

macroscopic

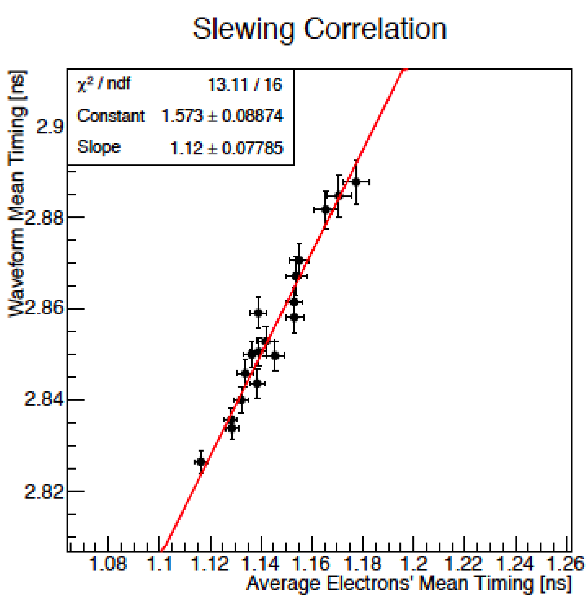

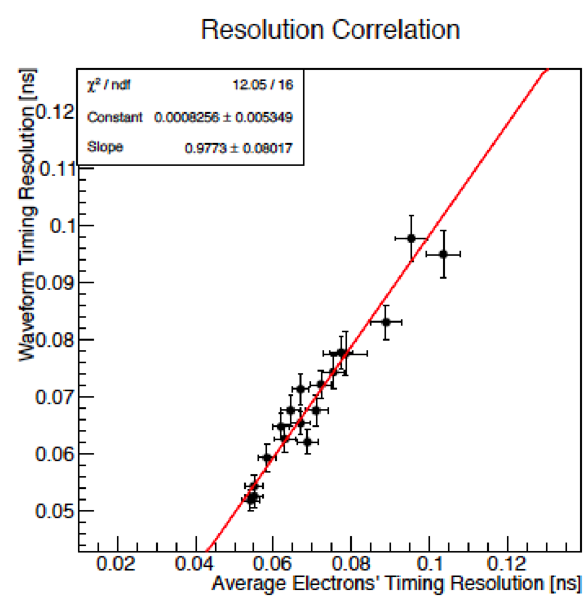

microscopic

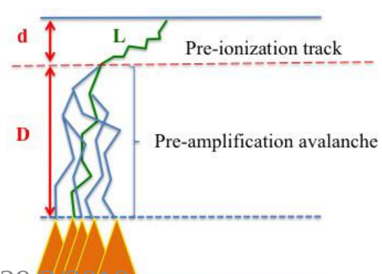

T is the mean value of all the electrons' arrival times at the mesh

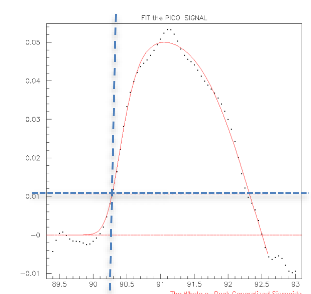

20% CFD

SAT

Total time (from the photocathode to the mesh)

Avalanche time (from the first interaction point to the mesh)

Photoelectron Time (from the photocathode to the interaction point)

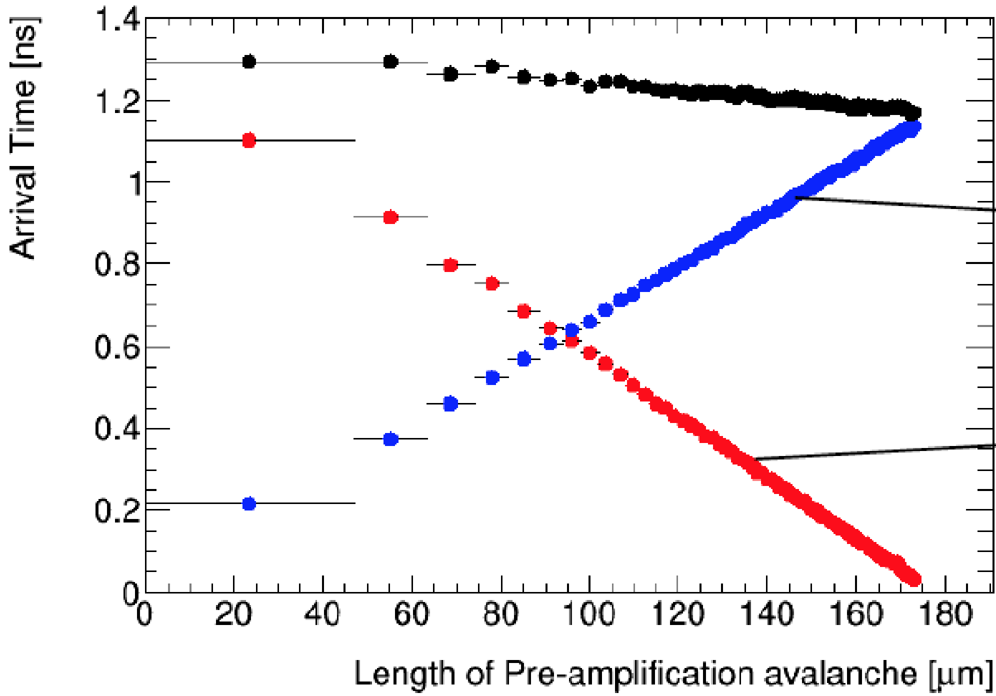

$$slope = \frac{1}{v} = \frac{1}{153.94\,\mu m/ns}$$

$$slope = \frac{1}{v} = \frac{1}{134.34\,\mu m/ns}$$

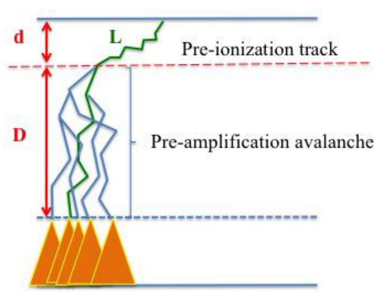

How is it possible the photoelectron and the avalanche to have different drift velocities?

Let us be inspired by the phenomenon of "Quenching"

From Rob Veenhof

Electrons in Ar/CO_2 at E=1 kV/cm

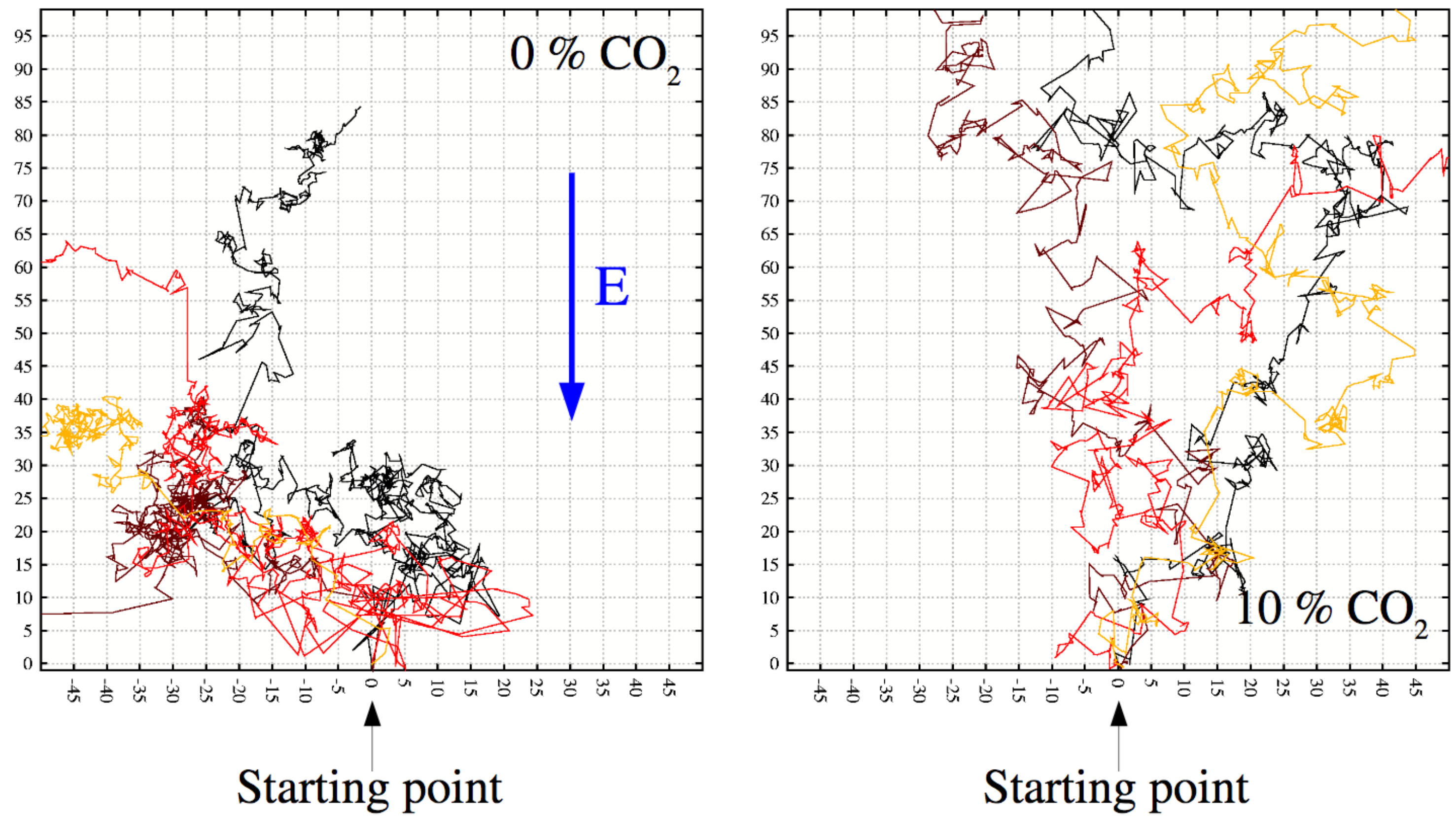

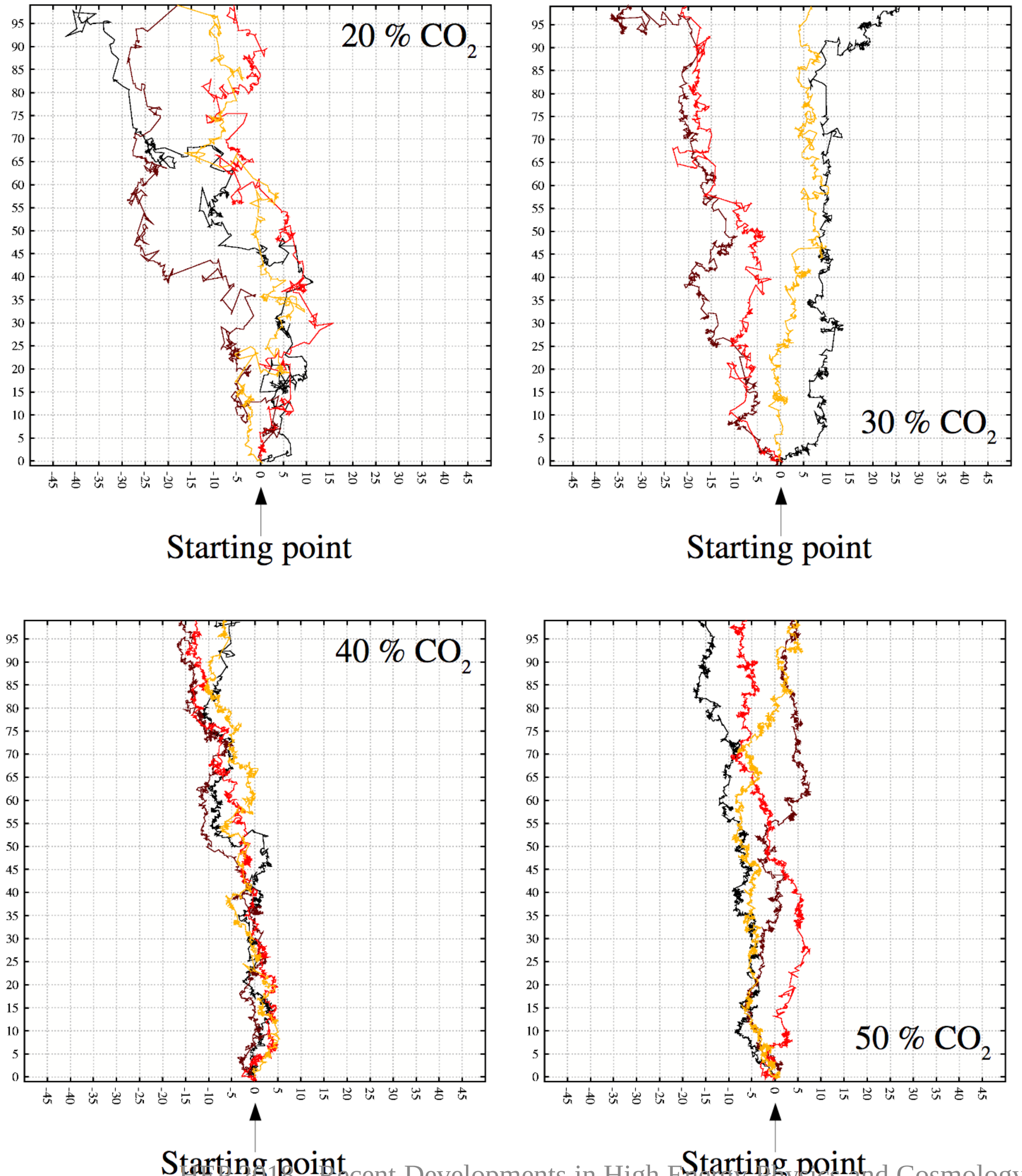

From Rob Veenhof

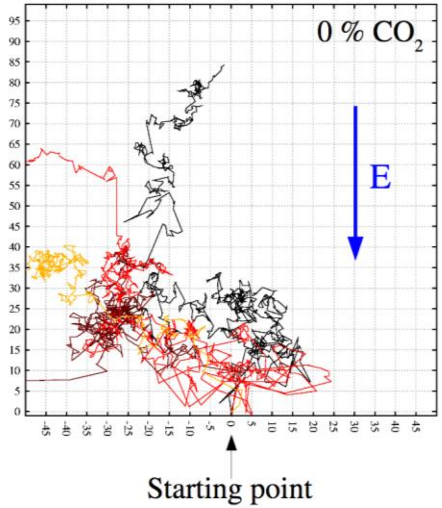

Elastic scatterings WITHOUT any significant energy loss

From Rob Veenhof

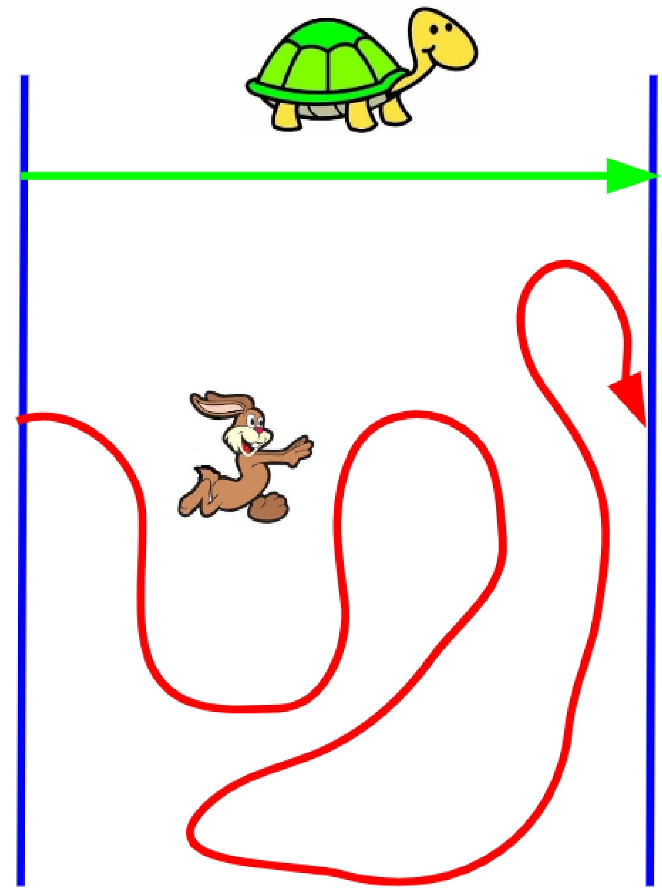

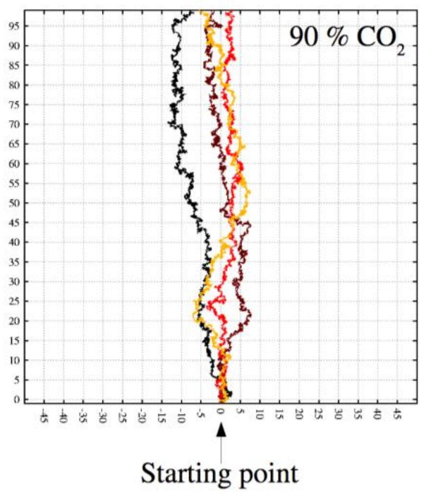

Scatterings WITH significant energy loss

•When the “ionization channel opens” the electrons in the avalanche loose energy
•As in the case of “quenching”, the energy loss results in higher drift velocity !!!
•Our model employs an effective parameter ρ that describes the “time gain due to the energy loss in each ionization (production of a new electron)
•The other parameters of the model are: the drift velocity of the photoelectron, the first Townsed coefficient and the attachment probability.
•The model treats the number of electrons in an avalanche as continues variable

We could predict the effective drift velocity of the avalanche

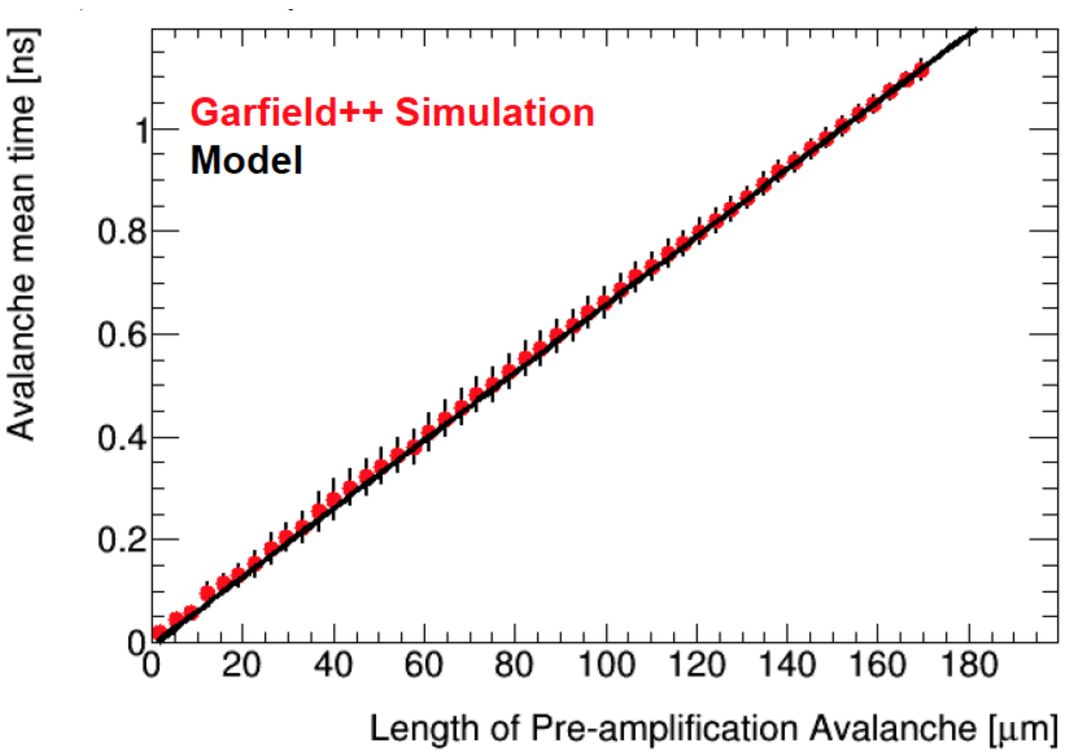

We could describe and explain the SAT dependence on the number of avalanche's electrons (i.e. on the e-peak size)

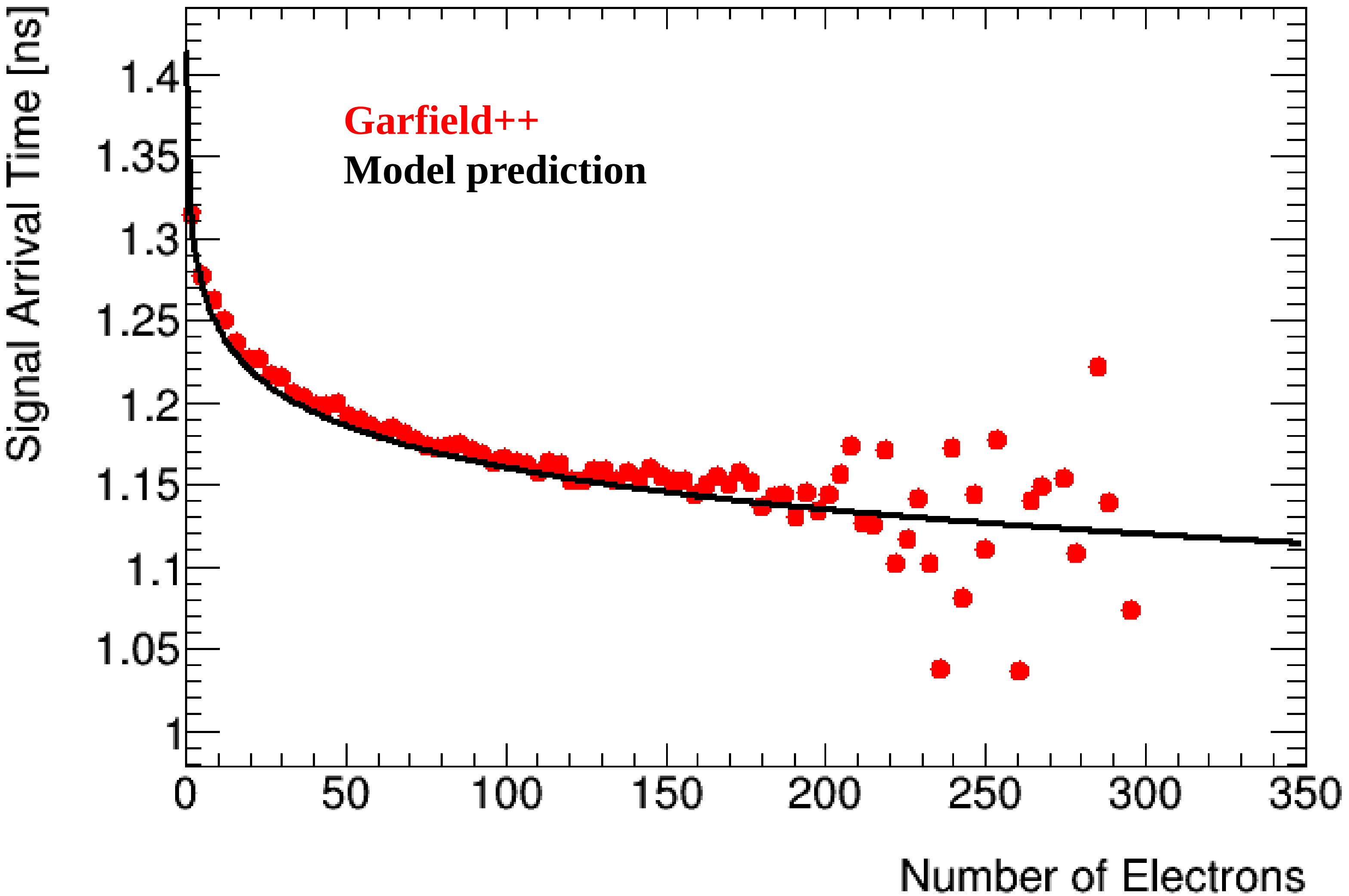

Points: Garfield++
Curves: Model Prediction

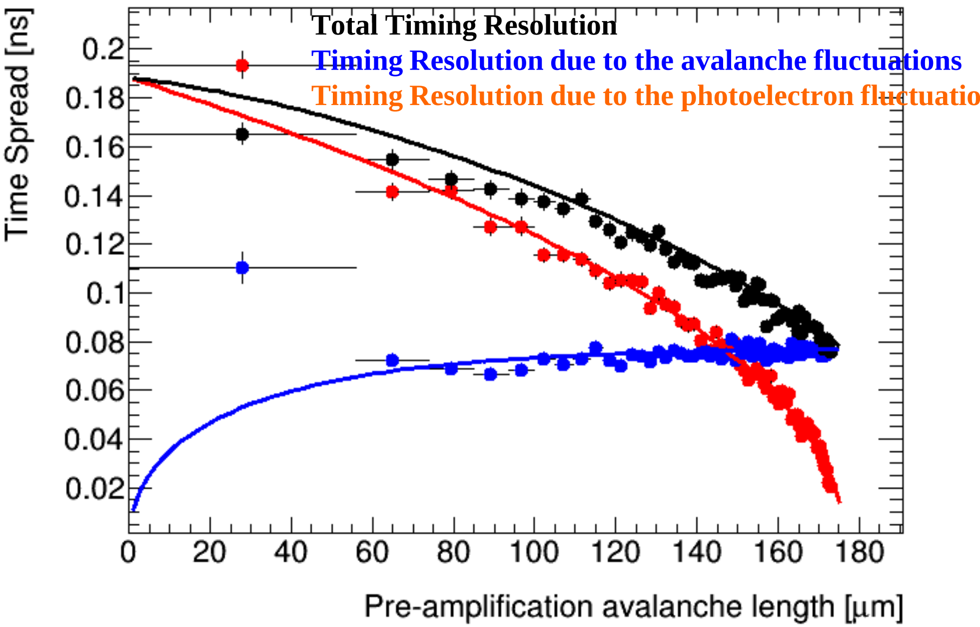

We could describe and explain the Resolution dependence on the length of the avalanche and on the number of avalanche's electrons (i.e. on the e-peak size)

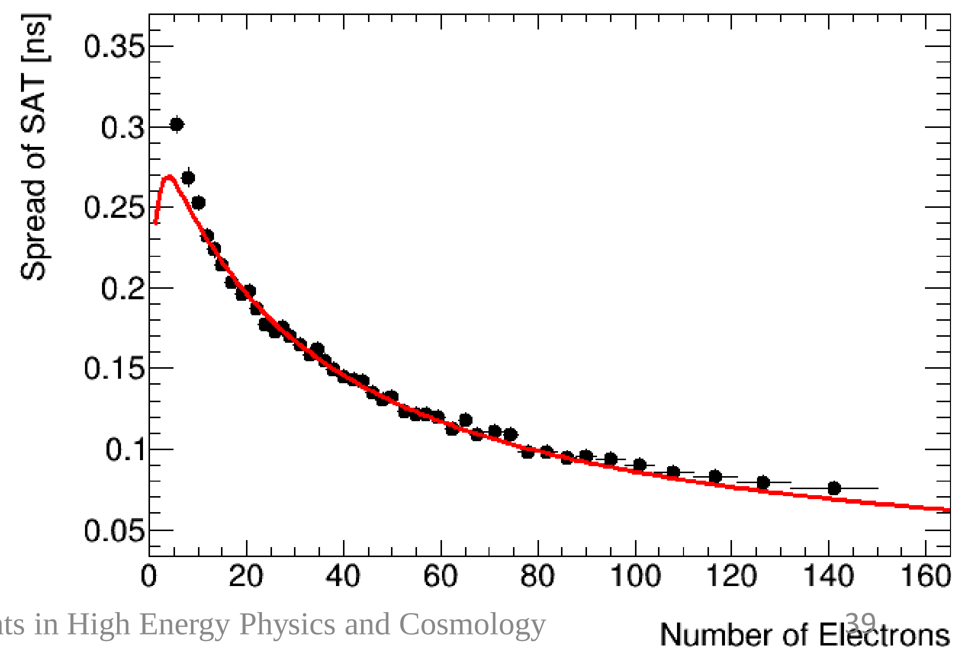

•We have developed the tools to describe the PICOSEC response and we have identify the major mechanisms which are responsible for the timing characteristics
•We can achieve less than 20 ps (15?) timing resolution with optimized working parameters (during the next test-beam period)
•We will run in intense laser beams, i.e. in similar conditions as in a electromagnetic calorimeter, to finalize the design of a calorimeter with ~1ps time resolution (Astroparticle Physics, Cosmology, Astrophysics…)
•We have operated a muli-pad PICOSEC detector. Very encouraging first results, data analysis is not finished. A new test-beam run in July

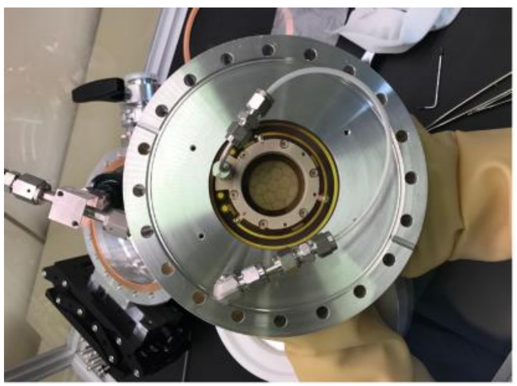

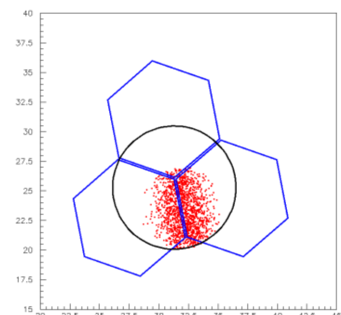

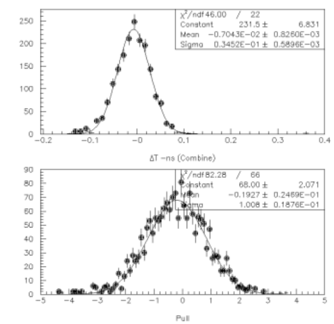

•We have started a detailed simulation study to evaluate the spatial resolution of several Micromegas tracker configuration with PICOSEC timing information. Many ideas… to be used as a demonstrator in the running LHC experiments
• PICOSEC applications for fire detection and early warnings

Resume

- The RD51 PICOSEC collaboration has developed a MicroMegas detector with photocathode and Cherenkov radiator
- First published results prove the potentiality of such a detector to perform precise timing of MIPs and single photons.
- I have presented studies to understand the underlying mechanism which are responsible for the timing characteristics.
- Further developments of the PICOSEC detector are currently investigated and will be tested in particle and laser beam

Thank you for your attention!!!